Studies on groundwater transport in fractured crystalline rock under controlled conditions using nonradioactive tracers

Erik Gustafsson
Carl-Erik Klockars

Geological Survey of Sweden, Uppsala, April 1981

STUDIES ON GROUNDWATER TRANSPORT IN FRACTURED CRYSTALLINE ROCK UNDER CONTROLLED CONDITIONS USING NONRADIOACTIVE TRACERS

Erik Gustafsson
Carl-Erik Klockars

Geological Survey of Sweden, Uppsala, April 1981

A list of other reports published in this series during 1981, is attached at the end of this report. Information on KBS technical reports from 1977-1978 (TR 121), 1979 (TR 79-28) and 1980 (TR 80-26) is available through SKBF/KBS.

STUDIES ON GROUNDWATER TRANSPORT IN FRACTURED CRYSTALLINE ROCK UNDER CONTROLLED CONDITIONS USING NONRADIOACTIVE TRACERS

Erik Gustafsson
Carl-Erik Klockars
Geological Survey of Sweden, Uppsala
April 1981

TABLE OF CONTENTS

SUMMARY

KBS (the Nuclear Fuel Safety Project) has commissioned SGU (the Geological Survey of Sweden) to study transport mechanisms in crystalline bedrock within the Finnsjö field research area with the aid of certain tracers.

The purpose of the investigation has been to study the following parameters along existing fractures between two boreholes:

- o Hydraulic properties of rock mass and fractures
- o Adsorptive properties of some selected tracers during transport along fractures
- o Dispersivity and diluation of tracers during transport in fractures
- o Kinematic porosity of fractured bedrock

The procedure has been to determine the hydraulic properties of a rock mass by means of conventional hydraulic testing methods in 100 m deep boreholes, and to study transport mechanisms and properties of selected tracers in a selected fracture zone between two boreholes.

In summary, hydraulic tests and tracer experiments reveal the following with regard to the hydraulic parameters of hydraulic conductivity and kinematic porosity:

- o The studied fracture zone has a hydraulic conductivity of $2\text{-}3 \cdot 10^{-3}$ m/s, and its constituent main transport zones (representing about 90% of the total flow in the fractured zone) have a hydraulic conductivity of $3\text{-}5 \cdot 10^{-3}$ and $1\text{-}2 \cdot 10^{-3}$ m/s, respectively.

- o Kinematic porosity, calculated as the ratio between the hydraulic conductivities of the rock mass and the fracture zone, is $8\text{-}9 \cdot 10^{-4}$

- The roughness fractor β, which expresses the ratio between measured and calculated (plane-parallel) fracture conductivity, is approximately 0.2

- Calculations of fracture width give varying values depending upon the calculation method used. Water quantity calculations give approximately 20 times greater width than transport velocity calculations. The latter calculations give a fracture width of about $7 \cdot 10^{-5}$ m (0.07 mm)

The results and conclusions of comparison between the tracers Rhodamine WT, NO_3^-, I^-, Br^- and Cr-EDTA give the following:

- Rhodamine WT shows a weak retardation and sorption compared with NO_3^- and I^-
- I^-, NO_3^- and Cr-EDTA appear to be comparable as non-reactive tracers
- Br^- exhibits lower recovery in comparison with NO_3^- and I^-
- The natural occurrence of NO_3^- and Br^- can, in some cases, cause difficulties in interpreting results where NO_3^- and Br^- are used as tracers

In summary, the tracer tests with radial flow show the following with regard to dilution and dispersion:

- The studied fracture zone consists of at least two transport pathways with different hydraulic characteristics
- The dispersivity of the two transport pathways is 0.9 - 1.2 m
- Dispersivity calculated for the entire fracture zone (macrodispersivity) is approximately 10 times greater than for the individual transport pathway

- The dilution of the tracer in the case of instan taneous injection is mainly dependent upon the flow geometry and less on dispersion and dilution in the pump well
- The dilution due to hydrodynamic dispersion has been calculated to be about 1:9 (calculated for peak values).

1. BACKGROUND

In crystalline bedrock, the movement of the groundwater is chiefly dependent upon existing fractures and cruched zones. Substances dissolved in the groundwater are transported in fractures and crushed zones, but the transport is affected by factors associated with the properties of the solid rock in relation to the dissolved substances. Knowledge of these transport mechanisms in crystalline rock constitutes a very important part of the safety analysis of the problems associated with the storage of nuclear waste in the Precambrian bedrock. One of the feasibilitys for studies of these mechanisms is the tracer method. A tracer is injected into the groundwater and its transport in time and space is studied by means of direct measurements in the field or the taking of water samples.

The nuclear Fuel Safety Project, KBS, has commissioned the Geological Survey of Sweden, SGU to study transport mechanisms in crystalline bedrock within the Finnsjö field research area with the aid of certain tracers.

Otto Brotzen took the initiative to this investigation.

2. PURPOSE AND SCOPE

The purpose of the present investigations is to study and quantify the transport of certain tracers with the groundwater in crystalline bedrock under controlled conditions in the field.

The particular purpose of the study being carried out within the Finnsjö field research area in northern Uppland County is to study the following parameters along existing fractures between two boreholes:

- Hydraulic properties of the rock mass and fractures
- Adsorptive properties of some selected tracers during transport along fractures
- Dispersivity and dilution of tracers during transport in fractures
- Kinematic porosity of fractured bedrock

The study has comprised three main parts:

- Hydraulic tests to shed light on the hydraulic conductivity of the bedrock and the fractures
- Tracer tests with both instantaneous and continuous injection
- Evaluation, comparisons and preparation of the report

Extensive geological, hydrogeological and hydrological studies have been and are being conducted within the field research area aside from the present investigation in order to gain a further understanding of groundwater transport and groundwater turnover time in crystalline bedrock. These studies are being conducted with other goals and time perspectives, but their results have also been used in the present study.

3. THEORY

3.1 Groundwater flow and groundwater transport

3.1.1 Porous homogeneous media

The flow of groundwater in a porous medium can be expressed by Darcy's Law:

$$\frac{Q}{A} = k \cdot I \qquad (1)$$

where $\frac{Q}{A}$ = groundwater flow per unit area perpendicular to the transport direction
k = hydraulic conductivity of the medium
I = hydraulic gradient

The average transport velocity of the groundwater, can be calculated when the effective porosity of the formation is known. The effective porosity of a porous homogeneous medium is the ratio between the volume available for groundwater transport and the total volume, expressed as a decimal fraction. The average transport velocity is then obtained from the expression

$$\bar{v} = \frac{Q}{A \cdot \theta_e} \qquad (2)$$

where $\bar{v}$ = average transport veolocity of groundwater
θ_e = effective porosity

3.1.2 Fractured media

Groundwater flow in fractured media is usually approximated to flow in porous media. The validity of this approximation is determined by the scale factor. The scale factor includes the ratio between block size and considered volume and the orientation and distribution of fracture and crushed zones.

Theories have been developed for flow in individual fractures. Groundwater flow in fractured rock can be regarded as flow in plane-parallel apertures of infinite extent (Snow 1968).

The hydraulic conductivity, k_j, of a plane-parallel aperture of width e is obtained from the expression

$$k_j = \frac{e^2 \cdot g}{12 \cdot \nu} \qquad (3)$$

The flow with Darcy's Law is then

$$Q_j = k_j \cdot e \cdot w \cdot I = \frac{e^3 \cdot g}{12 \cdot \nu} \cdot w \cdot I \qquad (4)$$

where w = unit width
g = acceleration due to gravity
ν = kinematic viscosity

The hydraulic conductivity, k_p, measured in a rock mass constitutes the sum of the conductivities of constituent fractures and the matrix. Under the assumption that the constituent fractures are of uniform width and frequency, the conductivity of the rock mass can be obtained from the expression

$$k_p = \frac{1}{b} \cdot (e \cdot k_j + (b-e) \cdot k_m) \qquad (5)$$

where k_p = hydraulic conductivity of rock mass
b = fracture spacing
e = fracture width
k_j = hydraulic conductivity of fractures
k_m = matrix conductivity

Since $k_j >> k_m$ and $b > e$, if $\frac{1}{b}$ = the fracture frequency, n, (i.e the number of fractures per metre), the expression above can be approximated with

$$k_p = n \cdot e \cdot k_j \qquad (6)$$

Thus, under the given conditions, the hydraulic conductivity of the rock mass is a function of fracture frequency, fracture width and the hydraulic conductivity of the fractures.

In naturally occurring fractures, however, the flow is not to be regarded as plane-parallel, owing to the irregularity of the fracture plane. As a result, the calculated fracture conductivity, k_j, must be adjusted for the measured hydraulic conductivity, k_e, of a fracture zone:

$$k_e = \beta \cdot k_j \qquad (7)$$

The ratio between the measured hydraulic conductivity of a fracture zone, k_e, and the conductivity of the rock mass, k_p, is the ratio between the gross velocity of the water and its velocity in the individual fracture, providing that Darcy's Law applies and that the gradient is equally large over the rock mass and over the fracture. This ratio is called the kinematic porosity, θ_k, and strictly expresses the portion of the rock mass available for water transport.

$$\theta_k = \frac{k_p}{k_e} \qquad (8)$$

3.1.3 Radial flow in two-dimensional geometry

In tracer tests with radial flow, the gradient and thereby the velocity is not constant along a flow line. In the field tests, the average travel time of a non-reactive tracer is determined from the breakthrough curve for transport from the point of injection to the point of detection. On the basis of two-dimensional radially symetrical laminar flow, the hydraulic conductivity is calculated as follows: (personal, communication J. Stokes 1979)

$$k_e = \frac{\ln (r_b/r_a)}{2\, t_o} \cdot \frac{r_b^2 - r_a^2}{\Delta h} \qquad (9)$$

where k_e = hydraulic conductivity
r_b = distance from injection hole to observation hole
r_a = radius of pump hole
t_o = mean transit time
Δh = difference in head between injection hole and pump hole

The average velocity, $\bar{v}_r$, over the distance r from the pump hole is given by

$$\bar{v}_r = \frac{1}{r} \cdot \frac{\Delta h \cdot k_e}{\ln (r/r_a)} \qquad (10)$$

where Δh = difference between the head of the groundwater in the pumphole and at a distance r

The equations are valid for flow in plane-parallel fractures as well as in porous media.

3.2 Dispersion

A water-soluble substance that is transported with the groundwater will be spread in time and space. This spreading, which occurs both in the flow direction of the groundwater and perpendicular to this direction is called dispersion. In relation to the average transport velocity of the groundwater, the dispersion will cause some of the dissolved substances to be transported more slowly and some faster than the average groundwater velocity.

The dispersion is dependent upon two factors:

- the velocity distribution in the medium
- molecular diffusion

The portion of the dispersion that is dependent upon the velocity distribution in the groundwater-bearing medium is termed mechanical dispersion. Mechanical dispersion of a water-soluble substance thus requires groundwater flow in a medium with a system of pores or channels.

Molecular diffusion is caused by differences in the concentration of the water-soluble substances in the groundwater. Molecular diffusion thus leads to a dispersion even if the groundwater does not have any velocity and takes place from areas of high concentration to areas of low concentration of the dissolved substance. The velocity with which a substance diffuses is dependent upon the concentration gradient and a diffusion constant D_m. This constant is in turn dependent upon the particular water-soluble substance in question (Neretnieks 1977 and 1978). For substances of low molecular weight, $D_m \approx 1 - 5 \cdot 10^{-9}$ m^2/s. Molecular diffusion follows Fick's Law.

$$V_F = -D_m \cdot \frac{\delta C}{\delta x} \cdot a \qquad (11)$$

where V_F = velocity of molecular diffusion rate

$\frac{\delta C}{\delta x}$ = concentration gradient of the substance

a = constant

Depending upon whether the groundwater-bearing medium is inhomogeneous on a microscopic or macroscopic scale, the dispersion is termed microdispersion or macrodispersion.

In principle, the dispersion can be dealt with by means of two different approaches. In calculations for porous media, it is normally assumed that a gradual spreading takes place in accordance with a coefficient of dispersion and a change in the concentration gradient. This approach is the basis for the calculations reported in the present study. In the other approach, packages of the substance in question are assumed to be transported without spreading in parallel channels that are not in contact with each other. In this case, the dispersion is dependent

upon the number of different channels or fractures and their properties. For further studies of this latter approach with applications, the reader is referred to Neretnieks (1980).

The general dispersion equation for one-dimensional flow of non-reactive substances is given by:

$$\frac{\delta C}{\delta t} = D \frac{\delta^2 C}{\delta x^2} - \bar{v} \frac{\delta C}{\delta x} \qquad (12)$$

where C = concentration of the non-reactive substance in the groundwater
D = longitudinal dispersion coefficient
$\bar{v}$ = average transport velocity of the groundwater
x = coordinate in flow direction
t = time variable

3.3 Retardation

3.3.1 General

The concentration distribution in the groundwater of a water-soluble substance that is transported in porous or fractured media is affected not only by dispersion, but also by chemical and physical processes such as

1) diffusion into the medium's matrix
2) ion exchange
3) adsorption
4) reversible precipitation
5) irreversible reactions with the medium
6) complex formation
7) filtration effects

The degree to which these processes affect the concentration distribution is dependent upon, among other things:

- o the chemical-physical state of the groundwater
- o properties of the groundwater-bearing medium
- o properties and initial concentration of the water-soluble substance

The aggregate effect of the processes (2), (3), (4) and (5) is termed sorption.

Both diffusion and sorption retard the transport of the substances in the groundwater. This retardation can be expressed by means of the retention factor R, which designates the ratio between the transport velocity of the groundwater $\bar{v}$ and the velocity of the water-soluble substance $\bar{v}_R$ according to

$$\bar{v} = R \cdot \bar{v}_R \qquad (13)$$

3.3.2 Diffusion

A water-soluble substance diffuses not only within the groundwater (Section 3.2) but also into the matrix of the groundwaterbearing medium, as illustrated in Figure 3.3.2a. This is specially true in crystalline rock, where porosity and thereby the transport of dissolved substances is dependent upon the presence of macro- and micro-fractures. All existing fractures are not interconnected or are of such small width that the water in these fractures cannot move under prevailing hydraulic conditions. According to Norton and Knapp (1977), porosity can be broken down into

$$\theta_T = \theta_k + \theta_d + \theta_r \qquad (14)$$

where θ_T = total porosity
θ_k = kinematic or flow porosity
θ_d = diffusion porosity
θ_r = residual porosity

Of the above-mentioned porosities, kinematic porosity constitutes the portion of the rock volume through which water can flow. Fig. 3.3.2b illustrates schematically the possible interrelationships between the different fractures, where the fractures marked with arrows constitute the space available for water flow.

The diffusion porosity represents the portion of the pores that exist between continuous water-conducting fractures and that are in contact with them, see Fig. 3.3.2b. However, this contact is so hydraulically limited that water flow is not possible out of or into these fractures. In other words, the width of the fractures is too small and/or the fractures lack continuity with each other. Nevertheless, the transport of water-soluble substances through diffusion is possible provided that concentration gradients exist and that the molecular size of the substances is smaller than the width of the fractures.

The diffusion process proceeds in the opposite direction to the concentration gradient, which also means that the substance can migrate from the matrix to the groundwater when its concentration is greater in the matrix than in the groundwater. This causes a retardation and "tail effect" of the transport of the water-soluble substance with the groundwater, which varies depending upon the microfractures in the rock and the substance in question.

3.3.3 Sorption

The sorption of a substance generally increases as the concentration of the substance in solution increases. At equilibrium, the relationship between the quantity that is sorbed by the medium and the concentration of the substance in solution is described by empirical relationships termed sorption isotherms. The most common types of isotherms are Freundlich and Langmuir isotherms, which are expressed mathematically as follows:

$$M = a \cdot C^n \qquad \text{(Freundlich)} \qquad (15)$$

$$M = \frac{b \cdot C}{1+b \cdot C} \cdot M_m \qquad \text{(Langmuir)} \qquad (16)$$

where M = quantity of sorbed substance per unit weight of the groundwaterbearing medium at equilibrium

C = concentration of the substance in solution at equilibrium

M_m = quantity of sorbed substance per unit weight required to form a monolayer on the surface of the medium

a,b,n = constants for respective system of substance and material

At equilibrium, the proportion between the quantity in solution and the quantity that is sorbed by the medium is given by a distribution coefficient that is related to the volume or the surface area of the groundwaterbearing medium.

The distribution coefficient K_d is related to the volume and is given by

$$K_d = \frac{M}{C} \qquad (17)$$

The distribution coefficient K_a is related to the surface area of the medium with which the water-soluble substances are in contact during transport with the groundwater and is given by

$$K_a = \frac{K_d}{A_m} = \frac{K_d \cdot \delta}{a} \qquad (18)$$

where A_m = specific surface area

a = specific surface area

δ = bulk density of the medium

At low substance concentrations and low transport velocities, it is often preferable to use the previously mentioned retention factor, equation (13), to describe the transport velocity. If the retardation is dependent solely upon sorption, the retention factor, R, can be calculated from the distribution coefficient, and the transport velocity of a water-soluble substance is given in relation to the transport velocity of the groundwater as follows:

$$\bar{v}_R = \frac{\bar{v}}{R} = \frac{\bar{v}}{1 + K_d \cdot \delta \cdot \frac{(1 - \theta_k)}{\theta_k}} \qquad (19)$$

or

$$\bar{v}_R = \frac{\bar{v}}{R} = \frac{\bar{v}}{1 + K_a \cdot a \cdot \frac{(1 - \theta_k)}{\theta_k}} \qquad (20)$$

where θ_k = kinematic porosity

4. TEST AREA

4.1 General description

The Finnsjö field research area, situated east of Lake Finnsjön in northern Uppland county (140 km north of Stockholm), constitutes an approximately 25 km^2 large catchment area, see Fig. 4.1a. Annual precipitation is about 685 mm (corr.) and evaporation is eastimated at about 475 mm. The topography is relatively flat, with levels between 20 and 44 metres above sea level. The loose deposits, which consist mainly of glacial moraine (till), are of small thickness, for the most part. The portion of exposed rock is relatively high, nearly 20%. The bedrock is of the Precambrian crystalline type, with a young granite and granodiorite in the central parts of the area. Leptite occurs in the southern and northern parts of the area, as well as deep greenstone in the northern part.

The geology, hydrology and groundwater conditions of the field research area have been described by Almén et al (1979), Olkiewicz et al (1979) and Scherman et al (1978), among others.

4.2 Test site

4.2.1 Geology and topography

The test site is situated in the northwestern portion of the Finnsjö area adjacent to a crushed zone at Gåvastbo, see Fig. 4.2.1a. The crushed zone runs in an approximate north-north-westerly direction, its dip is steep and the crushed zone recurs in the core of borehole Fi 8 as a number of parallel-displaced fracture zones.

Ten approximately 100 m deep hammerdrilled boreholes and two 460 - 730 m long cored boreholes have been drilled within the test site. Fig. 4.2.1a shows the location of the boreholes and a schematic map of the test site. The

test site can be described as a block of bedrock bounded in the east by the crushed zone at Gåvastbo and in the north and south by smaller east-westerly marked fracture zones.

The outcroping block consists of a relatively well exposed area, with for the most part deforested ground. The depression along the crushed zone east of the outcrop is dominated by farmland,planted with trees,with small outcroppings. In the depression, the loose deposits are approximately 5 m at the thickest. The rock is overlain by moraine, then clay and on top a thin layer of peat.

The rock, mapped on the surface as well as on the core of borehole Fi 8, consists for the most part of a grey, mediumgrained gneissgranitic rock of granodioritic-granitic composition. The gneissgranite is banded with occasional, irregular veins of pegmatite and aplite, normally only up to 0.2 m wide. Quartz occurs in isolated veins and in places as fracture filling. The most common fracture fillings are chlorite, calcite and pyrite.

4.2.2 Groundwater conditions

The natural groundwater flow within the test site presumably follows the topography, i.e. a flow from the outcroping block towards the depression at Gåvastbo. Water pressure tests in existing boreholes indicate a downward-directed groundwater transport within the outcroping block, with an upward-directed flow of groundwater in the crushed zone. Taken together, these observations give a picture of a three-dimensional groundwater flow with the inflow area comprising the outcroping block and an outflow area in the depression along the existing crushed zone. A more or less horizontal groundwater flow is believed to prevail along the depression and in the upper parts of the crushed zone.

4.2.3 Hydrochemical enviroment

The results of the water analyses that have been carried out within the test area are summarized in tables 4.2.3a and 4.2.3b. The high chloride and sulphate contents suggest the influence of relict seawater; in general, the water can be said to have high total salinity.

Groundwater that has infiltrated in forested areas can be expected to have low nitrate levels. In borehole G1, which lies in the depression, occassionally high nitrate concentrations are found. The high levels and the wide variation of nitrate concentrations with time indicate the admixture of superficial groundwater. Water is pumped continuously from borehole G1, with a drawdown of about 8 m below the top of the pipe. Water leaks in from the Quaternary deposits at the 4 m level. The high nitrate concentrations in the borehole probably derive from this leakage, see Table 4.3.2a.

Loggings of pH, Eh and the conductivity of the borehole liquid in cored boreholes Fi 6 and Fi 7 within the Finnsjö field research area (Duran & Magnusson, 1980) show Eh values between -60 and -120 mV at a depth of 50 - 100 m. This means that reducing conditions prevail. A good correlation between increasing conductivity and decreasing Eh and between increasing pH and decreasing Eh is obtained in the core boreholes.

The tracer experiments were carried out in the local outflow area in the depression between boreholes G2, section 91 - 93 m, and G1, section 100 - 102 m.

The results of the water analyses from boreholes G1, G2, G5 and G10 in the depression, table 4.2.3a, show high conductivities and high pH values, which, considered together with the fact that they are located in an outflow area, should mean reducing conditions at depth in these boreholes.

Table 4.2.3a Results of water analyses performed within the test area

		G1[1] 780413	G1[1] 780711	G1[1] 780830	G1[1] 781026	G1 4 m 781111	G1[1] 800221	G1[1] 800229	G2 66 m 780227	G2 94 m 781030	G5 25 m 780704	G 10[1] 800221	G10[1] 800229
kond.	mS/m	198	255	205	230	210	280	280	190	135	135	216	211
pH		7.0	7.45	7.4	7.5	7.45	8.1	8.3	8.0	7.6	8.25	8.2	8.3
$KMnO_4$ elof	mg/l	27	21	20	32	24	30	31	27	25	15	26	24
tot hårdhet Ca	"	180	204	176	181	160	198	201	126	76	140	152	156
Ca	mg/l	152	168	148	146	132	161	161	99	61	105	126	133
Mg	"	17	22	17	21	17	21	21	16	9	21	15.5	13.5
Na	"	265	355	315	330	320	390	420	280	240	275	320	300
K	"	2.7	4.3	3.8	4.1	3.5	4.0	4.0	4.3	3.1	4.2	5.8	5.3
Cl	mg/l	577	720	620	635	600	716	724	445	330	600	540	524
SO_4	"	47	55	53	52	34	55	60	54	20	29	42	42
HCO_3	"	198	260	251	268	266	282	290	320	285	305	235	233
NH_4	mg/l	0.17	< 0.01	0.17	0.20	0.01	0.09	0.27	0.50	< 0.01	0.09	0.17	0.15
NO_2	"	< 0.01	< 0.01	0.15	< 0.01	< 0.01	0.66	0.01	< 0.01	< 0.01	< 0.01	0.05	0.01
NO_3	"	0.14	1.80	1.20	0.44	0.92	1.4	0.1	0.11	0.63	0.07	0.1	0.3
PO_4	"	< 0.01	< 0.01	< 0.01	< 0.01	0.01	0.01	0.02	< 0.01	0.02	0.01	0.03	0.01
tot Fe	mg/l	0.18	0.86	0.10	1.07	1.10	0.36	0.05	0.64	2.3	0.29	0.23	0.23
Fe elof	"						0.02	0.04				0.04	0.02
Mn	"	0.30	0.24	0.24	0.18	0.22	0.26	0.27	0.22	0.11	0.06	0.16	0.16
F	mg/l	1.1	2.3	2.3	2.2	1.8	1.5	1.6	2.2	3.1	3.6	1.4	1.4
SiO_2	"	11.8	14	14	14	12	13	13	11.2	13	13	11	11
TOC	"	6.8	5.8	6.4	5.5	7.2	5.5	5.6	6.9	7.4	5.8	4.9	4.9

1) Pump water from all levels in the borehole

Table 4.2.3b Chromium and strontium concentrations in the water pumped out of borehole G1.

Datum	Krom	Strontium
790110		1.7 ppm
790915	0.01 ppm[x]	2.3 "
800221	< 5 ppb	
800229	< 5 "	
800331	< 5 "	
800507	< 5 "	
800508	< 5 "	
800717		2.3 "
800718		2.0 "

x) not measured with the same accuracy as later samples

5. TESTS PERFORMED

5.1 General

A large number of tests of both a general and a detailed nature have been performed within the Finnsjö field research area. The results of these tests provide the basic information that exists regarding the test area and the test site. In the present work, the following tests have been carried out for studies of hydraulic properties and groundwater transport:

- o Hydraulic tests
  - Water injection tests
  - Test pumping
- o Tracer tests under controlled conditions
  - Instantaneous tracer injection
  - Continuous tracer injection over a long period of time

5.2 Hydraulic tests

5.2.1 Water injection tests

Hydraulic conductivity was measured in sealed-off 2 m sections of boreholes G1 - G7 in accordance with the water injection method. The principle of water injection testing is that water is injected at constant pressure into a borehole or part thereof at the same time as the water flow is recorded. When the flow has stabilized, equilibrium is presumed to prevail and the calculations are performed under the assumption that a steady state exists. According to Moye (1967), hydraulic conductivity, k_p, for the measuring section can be calculated under these assumption as follows:

$$k_p = \frac{Q}{L \cdot H \cdot 2\pi} \cdot (1+\ln L/2 \cdot r_a) \qquad (21)$$

where k_p = hydraulic conductivity
Q = water flow
L = length of measuring section
H = excess water-pressure in measuring section
r_a = borehole radius

The sources of error in the calculation of hydraulic conductivity from water injection tests are both theoretical and practical. The size and influence of different sources of error were briefly dealt with in KBS Technical Report 79-06.

5.2.2 Test pumping

Test pumping was carried out in borehole G1. At the same time, changes in groundwater pressure were recorded in boreholes G2 - G7 in order to ascertain the hydraulic contact between the pump hole and other boreholes, see KBS Technical Report 60. In borehole G2, the pressure changes were recorded in section 91-93 m, which was sealed off by means of packer seals.

Test pumping was performed as step drawdown pumping, as indicated in table 5.2.2a. By step drawdown pumping means test pumping of a well at a constant capacity for a given period of time, after which the capacity is increased to a new constant higher value, which is maintained during the next step.

Table 5.2.2a Pump capacities and times for step drawdown pumping of borehole G1.

Pump step	Capacity (l/s)	Time (h)
1	0.1	1
2	0.2	1
3	0.4	20

The results of test pumping were evaluated according to Jacob's method, whereby hydraulic conductivity, k_D, and the storage coefficient, S, were calculated.

5.3 Tracer tests under controlled conditions

5.3.1 Method and tracers used

The purpose of the tracer tests referred to in section 2 was to determine the properties of the medium (the fractures), the usefulness of the selected tracers in crystalline bedrock and travel times for the tracers under controlled conditions. The results of hydraulic tests and measurements of groundwater head were used as a basis for the selection of a fracture zone for the tracer tests.

The goundwater level in borehole G1 was lowered by continuous pumping at constant capacity. By this means, controlled groundwater conditions were obtained within a given radius with a groundwater flow towards borehole G1.

The fracture zone between boreholes G1, section 100-102 m, and G2, section 91-93 m, was found to have the best developed hydraulic contact between the boreholes. Furthermore, this fracture zone was shown by injection tests in G2 not to have any contact with the rest of the borehole.

Tracer was injected into borehole G2, section 91 - 93 m, for later detection in the outgoing water flow from G1. The distance between the points of injection and detection is 30 m, see Fig. 5.3.1a. Altogether five tests were performed with instantaneous or continuous injection of tracer. The scope of the different tests and the tracers used are shown in table 5.3.1a.

Table 5.3.1a Tracer tests performed and tracers used in tests between boreholes G2, section 91-93 m, and G1, section 100-102 m.

Test	Tracer	Injection technique	Injection concentration C_o	Notes
1	Rd WT	Instantaneous	166 ppm	
	NO_3^-		2 M	
2	Rd WT	Instantaneous	166 ppm	
	I^-		1 M	
3	Br^-	Instantaneous	2 M	
	NO_3^-		2 M	
4	Cr-EDTA	Continuous	200 ppm	
	I^-		$6.7 \cdot 10^{-2}$ M	
5	Sr^{2+}	Continuous	$9.4 \cdot 10^{-2}$ M	not reported
	I^-		$6.7 \cdot 10^{-2}$ M	

The tracers were detected in the laboratory in samples of pumped-up water. Ion-selective electrodes were used for the detection of nitrate, iodide and bromide ions. Rhodamine WT was detected with a fluorometer. Chromium and strontium were detected with an emission spectrometer, IDES (Danielsson & Lindblom, 1976). Prior to each test, a calibration curve was plotted for the tracer mixture in question diluted in pumpwater for determination of injection concentration and simultaneous check of the mutual influence of the tracers on detection accuracy.

5.3.2 Instantaneous injection of tracer

An injection should be carried out in such a manner that it disturbs the natural flow pattern as little as possible. However, a compromise must be struck between the amount of the disturbance and certainly that the tracer solution penetrates into the fractures. In tests with the instantaneous injection of tracers, the following procedure has been used.

Immediately prior to injection, groundwater is pumped up out of the borehole, section 91-93 m. The tracers are dissolved in some of this groundwater so that a tracer solution of three litres is obtained. The tracer solution is injected into the borehole, and then the remaining pumped-up groundwater.

According to Zuber (1974), tracer concentration as a function of time t in a pumped hole with instantaneous injection in another borehole at a distance x can be calculated with good approximation by means of equation (12), which applies for one-dimensional flow. In this case equation (12) has the following solution (Lenda and Zuber 1970, Kreft et al 1974):

$$C\ (x,\ t) = \frac{m}{V} \cdot \sqrt{\frac{1}{4 \cdot \Pi \frac{D}{vx} \cdot (\frac{t}{t_o})^3}} \cdot \exp \frac{-(1 - \frac{t}{t_o})^2}{4 \cdot \frac{D}{vx} \cdot \frac{t}{t_o}} \qquad (22)$$

where t_o = mean transit time of water

$\frac{D}{vx}$ = dimensionless dispersion parameter

m = total mass (activity) injected

V = total volume of the water-satured pores in which the water movements occur

In the case of an aquifer with cylindrical geometry, thickness h and effective porosity θ_e, the volume V is given by

$$V = \theta_e \cdot \Pi \cdot x^2 \cdot h \qquad (23)$$

Velocity in the case of radial flow is not constant, however, and equation (22) is therefore only valid for purely mechanical dispersion and where the dispersivity D/v can be assumed to be constant and molecular diffusion can be neglected (Zuber, 1974).

5.3.3 Continuous injection of tracers

In the case of continuous injection, a tracer solution of given concentration is injected into the fracture zone at a constant flow rate over a longer period of time. Injection of tracer is preceded by injection of groundwater for 2-3 days for adjustment of flow, at the same time as a state of equilibrium is developed in the head of the groundwater. The injection flow has been kept low ($2.7 \cdot 10^{-4}$ l/s) in order to minimize the local disturbance of the groundwater flow around the injection zone.

In the case of continuous injection with constant flow and tracer concentration, C_o, equation (12) for one-dimensional flow has the following solution (Ogata and Banks, 1961):

$$F\left(\frac{D}{vx}\ \frac{t}{t_o}\right) = \frac{C}{C_o} = \frac{1}{2}\left(\operatorname{erfc}\ \frac{1-\frac{t}{t_o}}{2\ \frac{D}{vx}\cdot\frac{t}{t_o}} + e^{\frac{v\cdot x}{D}}\cdot\operatorname{erfc}\ \frac{1+\frac{t}{t_o}}{2\cdot\frac{D}{vx}\cdot\frac{t}{t_o}}\right) \quad (24)$$

With radial flow and continuous injection in a borehole at a distance x from the pump hole, the same approximation applies as with instantaneous injection. Tracer concentration as a function of time t in the pump hole and dispersivity D/v can therefore be calculated from equation (24), which applies for one-dimensional flow.

6. RESULTS AND DISCUSSIONS

6.1 Hydraulic tests

Hydraulic conductivity measured in 2 m sections of boreholes G1 - G7 exhibits a wide spread, both between different measuring sections and between the different boreholes, see KBS Technical Report 60. In the boreholes studied, hydraulic conductivity exceeds 10^{-6} m/s in 5% of the measuring sections. The results of the water injection tests for boreholes G1 and G2 are presented in Fig. 6.1a,b, where the calculated hydraulic conductivity for each 2 m section tested is reported as a function of length of the borehole.

The results of the step drawdown pumping of the fracture zone between pump hole G1, section 100-102 m, and observation hole G2, section 91-93 m, are presented in table 6.1a, where q represents estimated flow from the fractured zone, k_p hydraulic conductivity and S the storage coefficient calculated from the observation hole.

Table 6.1a Hydraulic parameters for fracture zone between G1 and G2.

Pump step	q (l/s)	k_p (m/s)	S
1	$4.6 \cdot 10^{-3}$	$4.7 \cdot 10^{-6}$	$1.0 \cdot 10^{-5}$
2	$7.4 \cdot 10^{-3}$	$4.0 \cdot 10^{-6}$	$5.8 \cdot 10^{-6}$

Hydraulic conductivity was measured by means of the water injection method in the 2 m section enclosing the fracture zone in G1 (section 100 - 102 m) and in G2 (section 91 - 93 m) and found to be $1.1 \cdot 10^{-6}$ m/s in the former case and $3.3 \cdot 10^{-6}$ m/s in the latter case. The discrepancy may have different explanations. According to Gidlund et al (1979), the water injection method should give a lower value for conductivity than the corresponding value obtained from a transient approach at high conductivities. Another explanation may be that the water

injection method gives point values from a fracture plane and that hydraulic conductivity can vary in different directions.

In water injection tests or test pumpings, hydraulic conductivity or transmissivity is determined for the borehole or a sealed-off portion of it. By regarding the fractures as plane-parallel apertures, a transition can be made from the hydraulic conductivity of the measuring section, according to equations (3) and (6), to calculating an equivalent hydraulic conductivity for a plane-parallel fracture in accordance with

$$k_j = \sqrt[3]{\frac{k_p^2 \cdot g}{n^2 \cdot 12 \cdot \nu}} \qquad (25)$$

where k_j = hydraulic conductivity of a plane-parallel fracture with laminar flow
k_p = hydraulic conductivity of the measuring section
g = acceleration due to gravity
n = fracture frequency
ν = kinematic viscocity

Calculations using equation (25) with n = 1 give a hydraulic conductivity, k_j, of the fracture zone of $1.4 \cdot 10^{-2}$ m/s.

6.2 Tracer tests

6.2.1 Presentation of results

The results of all tracer tests, both with continuous and with instantaneous injection, are reported as breakthrough curves in Figs. 6.2.1a-e. The time after injection is given on the horizontal axis and recorded concentration at the pump hole, related to injection concentration, on the vertical axis. In the case of continuous injection,

injection capacity and pump capacity are also taken into account. Recovery of the tracers is reported in the form of recovery curves in Figs. 6.2.1 f-h. The time after injection is given on the horizontal axis and the accumulated quantity detected at the pump hole, related to the injected quantity, on the vertical axis.

6.2.2 Comparison between tested tracers

An ideal tracer for studies of grundwater transport must follow the flowing water without being retarded or lost (see section 3), and must be reliably detectable even at very low concentration.

The tracers RdWT, NO_3^-, Br^-, I^- and Cr-EDTA were tested against each other by means of parallel injections in four testing rounds. The results are presented in table 5.3.1a. The experimental parameters were not exactly the same in the different tests. The tracers that were not tested against each other in the same tests can, however, be compared indirectly.

All tested tracers have been used frequently as non-reactive tracers in hydrogeological studies (Davis et al 1980). K_d determinations, see section 3.3, on drill cuttings from the Studsvik area, mainly with granitic gneiss, show K_d values close to zero for Br^- and I^- (Landström et al, 1978). This means that it is not meaningful to compare the tested tracers solely by means of the retention factor, R, calculated from equation (13).

The following results of the tracer tests are presented in table 6.2.2a:

- time of maximum concentration for breakthrough curves, t_p (peak time)
- dimensionless concentration at t_p
- recovery after three times t_p
- the retention factor R (calculated from t_p)

Table 6.2.2a Comparison of tracers in tests between boreholes G2 section 91 - 93 m and G1 section 100 - 102 m.

Test	Tracers	Injection technique	Peak time, t_p (hours)	Concentration at t_p (c/c_o)	Recovery at $3 \cdot t_p$ (%)	Retentation factor, R
1	RdWT	instantaneous	20.5	$1.30 \cdot 10^{-4}$	44	1.08
	NO_3^-		19	$2.26 \cdot 10^{-4}$	64	
2	RdWT	-"-	27	$1.06 \cdot 10^{-4}$	47	1.08
	I^-		25	$1.90 \cdot 10^{-4}$	67	
3	Br^-	-"-	18	$1.56 \cdot 10^{-4}$	55	
	NO_3^-		-	-	-	

Rhodamine WT was injected in the same quantity and at the same concentration in tests 1 and 2. The concentration peak, t_p, is only slightly later for RdWT than for NO_3^- and I^-. The retention factor, R, is also very close to one in both tests. The values of the concentration peak, however, is much lower for RdWT than for NO_3^- and I^-. This indicates that RdWT is more sorption-prone than NO_3^- and I^-. Sorption proneness is also indicated by the recovery curves, see Figs. 6.2.1 g-h. Rhodamine WT has a much flatter curve than NO_3^- and I^-.

By shifting the time axis for the recovery curves for NO_3^- and I^- - see Figs. 6.2.1 f,g - with the time difference between the peak time, t_p, of the reference RdWT between tests 1 and 2 (6.5 h), it is found that the recovery curves for NO_3^- and I^- are practically identical. The properties of NO_3^- and I^- relative to RdWT are shown in table 6.2.2b, which gives the ratios between I^- and RdWT and between NO_3^- and RdWT for concentration at peak time, t_p, and recovery at three times t_p.

Table 6.2.2b Ratios of concentrations at peak time, t_p, and recovery at three times t_p during tests 1 and 2.

Test	Tracers	Ratio between concentrations at peak time, t_p	Ratio between recoveries at $3 \cdot t_p$
1	I^-/RdWT	1.79	1.43
2	NO_3^-/RdWT	1.74	1.45

Table 6.2.2b and the recovery curves (Figs. 6.2.1f,g) show that the tracers NO_3^- and I^- have identical properties. In field tests, I^- has the advantage of occurring naturally in very low concentrations, normally below 0.01 ppm ($8 \cdot 10^{-8}$ M). Nitrate occurs naturally in larger quantities and has a naturally large variation in time and space, see section 4.2.3.

In test 3, there was such a wide spread of the NO_3^- values that only the very first part of the breakthrough curve gave any meaningful information. In the breakthrough curves for the Br^- and NO_3^-, the concentration increase comes at the same time and with the same slope. The direct comparison of recoveries in table 6.2.2a, however, shows lower recovery for Br^- then for NO_3^- and I^-. In natural waters, the Br^- concentration is on the order of 1/300 of the Cl^- concentration. As a result, within sites with the same type of hydrochemistry as the test area, high background levels of Br^- can be expected.

In test 4 with simultaneous continuous injection of Cr-EDTA and I^-, the breakthrough curves (Fig. 6.2.1d) are virtually identical. This indicates that Cr-EDTA is comparable to I^- as a non-reactive tracer in the enviroment in which the test was performed.

In summary, a comparison between the tracers Rhodamine WT, NO_3^-, I^-, Br^- and Cr-EDTA shows the following:

- o Rhodamine WT exhibits a weak retardation and sorption compared to NO_3^- and I^-
- o I^-, NO_3^- and Cr-EDTA are roughly comparable as non-reactive tracers
- o Br^- exhibits lower recovery than NO_3^- and I^-
- o A natural occurence of NO_3^- and Br^- can, in some cases, lead to difficulties in interpreting of results where NO_3^- and Br^- are used as tracers

6.2.3 Calculation of dispersivity and dilution

By fitting theoretically calculated breakthrough curves for both instantaneous injection and continuous tracer injection against corresponding experimental breakthrough curves, the mean transit time, t_o, and the dimensionless dispersion parameter D/vx, are obtained from equations (22) and (24).

Depending upon geometry and prevailing conditions, the calculated appearant concentrations are adjusted linearly to concentrations obtained experimentally. Possible reactions or effects of the tracer's contact with the rock mass are not taken into account in the calculations. Molecular diffusion is assumed to be negligible since it has little effect on total dispersion when the travel time is short (the velocity is high).

In connection with the transport of water-soluble substances in a non-homogenous medium, macrodispersion phenomena can occur. These phenomena are caused by the fact that transport of the tracer from the point of injection to the point of detection can take place in a larger number of fractures or channels with differing hydraulic properties. As a result, the breakthrough curve is more drawn-out than it would be if hydrodynamic dispersion alone were responsible for the appearance of the curve. The fracture zone between boreholes G2 (section 91-93 m) and G1 (section 100-102 m) that was studied in the tracer test turns out to consist of at least two distinguishable large transport

pathways. Figs. 6.2.3a and 6.2.3b exhibit two completely evaluated breakthrough curves for iodide with instantaneous injection on the one hand and continuous injection on the other. A similar pattern emerges: the breakthrough curve constitutes the sum of several partially superimposed breakthrough curves, of which only the two most prominent transport pathways have been analyzed. It is probable that additional transport pathways of lower dignity could be distinguished upon closer examination of the latter portions of the breakthrough curves.

The dimensionless dispersion parameter D/vx is obtained in the calculations, but since x = 30 m is constant in all tests, the dispersivity D/v is given in the table below.

The experimental parameters were not exactly the same on the different test occasions, which partly explains the differences in values obtained. In the case of instantaneous injection, the pulse of tracer solution forms a more or less circular disc of a given radius around the injection zone. This has an elevating effect on the dispersivity.

Table 6.2.3a Results of test with instantaneous injection of I^-

Parameter	Primary	Secondary
Mean transit time, t_{01}, t_{02}	30 h	62 h
Dispersivity, D/v	1.5 m	1.5 m

Table 6.2.3b Results of test with continuous injection of I^-

Parameter	Primary	Secondary
Mean transit time, t_{01}, t_{02}	25 h	91 h
Dispersivity, D/v	0.9 m	0.9 m

In the test with simultaneous continuous injection of I^- and Cr-EDTA, packer leakage caused perturbations of the breakthrough curve, so only the first steep rise of the breakthrough curve has been evaluated, see Figs. 6.2.3c,d. Cr-EDTA starts to come somewhat earlier and then reaches peak concentration at approximately the same time as I^-. This leads to a flatter curve with greater dispersivity, but a shorter average travel time. The differences are marginal, however.

Table 6.2.3c Results of test with continuous injection of I^- and Cr-EDTA

Parameter	I^-	Cr-EDTA
Mean transit time, t_{01}	38.5 h	37 h
Dispersivity, D/v	0.9 m	1.2 m

Dispersivity D/v can be regarded as a material constant (Koltz & Moser, 1974), so the fact that D/v is the same for both transport pathways is not surprising. In a given geological enviroment, the transport mechanisms along separate pathways are expected to be of a similar nature with statistical probability. Dispersivity D/v is a measure of heterogeneity. An estimate of longitudinal dispersion, D, calculated for the average velocity gives a value on the order of 10^{-4} m^2/s. The diffusion constant for a substance of low molecular weight is $D_m \approx 1\text{-}5 \cdot 10^{-9}$ m^2/s (Neretnieks 1977 and 1978). The assumption that the molecular diffusion can be neglected in the calculations can consequently be considered reasonable. In attempts to theoretically describe the breakthrough curve for continuous injection as consisting of only one transport zone, a value of D/v roughly one power of 10 higher was obtained, representing the macrodispersion. The curvefit was considerably worse, however.

Lenda and Zuber (1970) give the dispersivity values for fractured rock as being 10^0 - 10^2 m. The scale factor is of great importance for the dispersivity, so the high

values probably represent the macrodispersion. In tests with reactive as well as non-reactive tracers in granitic bedrock with 12 m between the injection and observation holes, Goblet et al obtained dispersivities on the order of 1 m. Using Br-82 as a tracer in a fracture zone with 51 m between the injection and observation holes, Landström et al (1978) give values of dispersivity of 7.8 m, probably dependent mainly on the macrodispersion.

Owing to dispersion, flow geometry and well effects as well as the injection procedure, a dilution of a non-reactive tracer is obtained. The different diluting factors have been considered separately and the following calculations have been used as a basis for quantification of the dilution.

In the case of instantaneous injection, the tracer solution will be pressed out into the fracture zone within a cylinder, which stands in proportion to the volume of the injection solution and the average fracture width of the injection zone. In tests with instantaneous injection of 3 l of tracer solution, this volume - with an estimated average fracture width of $1.65 \cdot 10^{-3}$ m (see section 6.2.4) - covers an area with a radius of 0.75 m around the injection hole. The ratio between the diametral propagation of the injection solution around the injection zone and the circumference of a circle with a radius of r_b = 30 m, with its centre in the pumped hole, constitutes the geometric dilution factor. This means that, when the tracer arrives at the pumped well, only a limited portion of the water flow from the fracture zone contains tracer. This dilution, which is dependent upon flow geometry, is estimated to be about 1:120 ($8.3 \cdot 10^{-3}$ C_o).

In the pumped well, the solution is diluted an additional 5 times when water flows in from other levels besides 100 - 102 m. Tests conducted in the pumped well show that the tracer's retention time in the well is somewhere around 4 hours and that D/vx in the well is much less than 0.01.

In table 6.2.3d, the dilution is given as the inverse of the concentration related to the original concentration.

Table 6.2.3d Dilution ratio at different times on the breakthrough curve with instantaneous injection of iodide, plus geometric dilution and well dilution.

	Peak value (t_p)	Mean transit time (t_o)	Geometric dilution	Well dilution
Dilution	$5.2 \cdot 10^3$	$1.0 \cdot 10^4$	$1.2 \cdot 10^2$	5

A comparison between the values obtained and the above-calculated dilutions shows that the dilution effect of the hydrodynamic dispersion, calculated on the peak value, should be about 1:9 ($0.12 \cdot C_o$), disregarding the effect of the initial dilution.

Makowski (comment on Lenda and Zuber 1970) has shown in laboratory tests with instantaneous injection that, for flat and cylindrical models of varying length, the tracer solution disperses exponentially with the transport distance as follows:

$$C_p = C_o \cdot e^{-a \cdot \sqrt{x}} \qquad (26)$$

where C_p = peak concentration
C_o = injection concentration
x = average transport distance

The coefficient, a, is dependent upon the dispersivity and physical-chemical factors.

In the tests with instantaneous injection of iodide, the factor a in equation (26) was determined to be on the order of 0.4 $m^{-1/2}$.

In connection with continuous injection, dilution at equilibrium is determined by the ratio of pump capacity to injection flow.

In summary, the tracer tests reveal the following with regard to dilution and dispersion:

- o The investigated fracture zone consists of at least two transport pathways with different hydraulic properties
- o Dispersivity for both of the transport pathways is 0.9 - 1.2 m
- o Dispersivity calculated for the entire fracture zone (macrodispersivity) is approximately 10 times greater than for the single transport pathway
- o The dilution of the tracer in connection with instantaneous injection is dependent for the most part on the flow geometry and to a lesser extent on dispersion and dilution in the pumped well
- o The dilution effect of the hydrodynamic dispersion has been calculated to be about 1:9 (figured on peak values)
- o The diffusion seems to have little effect upon dilution

6.2.4 Calculation of hydraulic conductivity and kinematic porosity

Hydraulic parameters were calculated from the breakthrough curves in accordance with theories presented in section 3. The hydraulic conductivity, k_p, obtained from water injection tests in the 2 m section enclosing the fracture zone tested in the tracer tests is given in table 6.2.4a as the average of the fracture zone's conductivity measured in boreholes G1 and G2. Table 6.2.4a also gives calculated values of the hydraulic conductivity of the fracture zone and the hydraulic conductivities of the transport pathways discussed in section 6.2.3. The calculation of the average

conductivity of the fracture zone, $\bar{k}_e$, is based on weighting of the mean transit times t_{o1} and t_{o2} in table 6.2.3 a,b against the partial curves' portion of the total curve in Figs. 6.2.3a,b.

Table 6.2.4a Calculated values of hydraulic conductivity for bedrock and fracture zone between boreholes G1 and G2. The calculations are based on water injection tests and tracer tests with instantaneous and continuous injection of iodide

Parameter		Water injection test	Tracer test	
			Instantaneous injection	Continuous injection
k_p	(equ 21)	$2.2 \cdot 10^{-6}$		
k_j	(equ 25)	$1.4 \cdot 10^{-2}$		
$\bar{k}_e$			$2.5 \cdot 10^{-3}$	$2.8 \cdot 10^{-3}$
k_{e1}	(equ 9)		$3.4 \cdot 10^{-3}$	$4.7 \cdot 10^{-3}$
k_{e2}	(equ 9)		$1.7 \cdot 10^{-3}$	$1.3 \cdot 10^{-3}$

The ratio between calculated hydraulic conductivity for the fracture zone from tracer tests, $\bar{k}_e$, and from water injection tests, k_j, constitutes the factor β in accordance with equation (7). Kinematic porosity, θ_k, is expressed as the ratio between the hydraulic conductivities of the rock mass and the fracture zone in accordance with the equation (8). Table 6.2.4b presents these calculated values.

Table 6.2.4b Calculated values of the factor β and kinematic porosity θ_k. Data from table 6.2.4a.

Parameter		Tracer tests with	
		Instantaneous injection	Continuous injection
β	(equ 7)	0.18	0.20
θ_k	(equ 8)	$8.8 \cdot 10^{-4}$	$7.9 \cdot 10^{-4}$

In previously referred two studies, Goblet et al as well as Landström et al obtain kinematic porosity on the order of $1 - 2 \cdot 10^{-3}$.

Evaluations from field tests can give varying values of kinamatic porosity, θ_k, for the same rock mass, depending upon how the tracer transport is studied: along the main fracture direction or more or less across it. It is consequently of great importance that the geometry of the fracture systems are known.

The width e of a plane-parallel aperture with hydraulic conductivity k_j can be calculated from equation (3). The fracture width can also be calculated with knowledge of the flow and travel times in the fracture plane. If it is assumed that no water is introduced into the fracture plane in the vertical direction within a radius of 30 m from the pump hole, fracture width e can be calculated as follows:

$$e = \frac{Q_s \cdot t_o}{\pi \cdot r^2} \qquad (27)$$

where t_o = mean transit time from tracer tests
Q_s = water flow from the fracture zone to the pumped well
r = radius (30 m)

The results of the two calculating methods are presented in table 6.2.4c.

Table 6.2.4c Calculated values of the width of the fracture zone between G1 and G2.

Calculating method	Tracer tests with I^-	
	Instantaneous injection	Continuous injection
Equ (3)	$6.8 \cdot 10^{-5}$ m	$7.2 \cdot 10^{-5}$ m
Equ (27)	$1.8 \cdot 10^{-3}$ m	$1.5 \cdot 10^{-3}$ m

The ratio between the different calculated fracture widths is 26 for instantaneous injection and 21 for continuous injection. It should be pointed out that the first calculation is based on the transport velocity and where the narrower sections of a fracture zone determine the water velocity. The latter calculation, which also gives the largest values, is based, on the other hand, on water quantities and the fact that, in this connection, water is most probably introduced into the fracture zone in a vertical direction.

In summary, the results of the hydraulic tests and tracer tests show the following with regard ro the hydraulic parameters of hydraulic conductivity and kinematic porosity:

- The fracture zone has a hydraulic conductivity of $2\text{-}3 \cdot 10^{-3}$ m/s and its main transport pathways has a hydraulic conductivity of $3\text{-}5 \cdot 10^{-3}$ and $1\text{-}2 \cdot 10^{-3}$ m/s respectively
- The kinematic porosity, calculated as the ratio between the hydraulic conductivities of the rock mass and fracture zone, is $8\text{-}9 \cdot 10^{-4}$
- The roughness factor β, which expresses the ratio between measured and calculated (plane-parallel) fracture conductivity, is about 0.2
- Calculations of fracture width give varying values depending upon the calculating method used. Water quantity calculations give roughly 20 times greater width than transport velocity calculations. The latter calculations give a fracture width of about $7 \cdot 10^{-5}$ m (0.07 mm).

7. CONCLUSIONS

The tracer tests performed in crystalline bedrock, in combination with hydraulic tests, provide a means of describing and quantifying the hydraulic properties of a selected fracture zone as well as, to some extent, its geometric parameters. The tests have shown that groundwater flow and transport mechanisms in an individual fracture zone can be described with good approximation by theories applicable to porous media, but with stratifications in the hydraulic conductivity of the media. In regarding groundwater flow on an intermediary scale, or when the geometry of the fracture zones is not known, however, the scale factor has an influence on validity of the approximation as a porous medium.

The studies of selected tracers, NO_3^-, I^-, Br^-, Rhodamine WT and Cr-EDTA were perfomred in different testing rounds with instantaneous and continuous simultaneous injection of two tracers. The tests revealed that there were no great difference in the reaction between the tracer studied and the medium, except in the case of Rhodamine WT, which exhibits some sorption. Evaluation of the breakthrough curves shows no appreciable difference in parameter determination between instantaneous and continuous injection.

Macro dispersion, which is dependent upon the flow pattern of the groundwater and the continuity and geometry of the fractures, is of the greatest importance for the dilution of a non-reactive tracer during transport in fractured media. The hydrodynamic dispersion related to the water velocity distribution in individual fractures appears to play a subordinate role in comparison with macrodispersion on the studied fracture system.

At the travel times applicable in the tests, diffusion appears to have a negligible effect on dilution.

Among the problems surrounding transport mechanisms in fractured media that require further study, the greatest emphasis should be given to studies of the effects of macrodispersion on dilution and dispersion and the effects of the scale factor on the approximation as a porous medium.

8. KEY TO SYMBOLS

A	(m^2)	area
A_m	(m^2/kg)	specific area
a	(m^2/m^3)	specific area
b	(m)	fracture spacing
C		concentration of water-soluble substance
D	(m^2/s)	longitudal dispersion coefficient
D_m	(m^2/s)	diffusion constant
$D/v \cdot x$		dispersion parameter
D/v	(m)	dispersivity
e	(m)	aperture width (fracture width)
g	(m/s^2)	acceleration due to gravity
H	(m.v.p)	excess water pressure
Δh	(m.v.p)	difference in groundwater head between two points
I	(m/m)	hydraulic gradient
K_a	(m^3/m^2)	distribution coefficient
K_d	(m^3/kg)	distribution coefficient
k	(m/s)	hydraulic conductivity
k_e	(m/s)	hydraulic conductivity calculated from travel time
k_j	(m/s)	fracture conductivity
k_m	(m/s)	hydraulic conductivity of matrix
k_p	(m/s)	hydraulic conductivity of rock mass
L	(m)	length of measuring section
n	(m^{-1})	fracture frequency
Q,q	(m^3/s)	flow
R		retention factor
r	(m)	radius
r_a	(m)	borehole radius
r_b	(m)	distance from injection hole to observation hole
S		storage coefficient
t	(s)	time
t_o	(s)	mean transit time
t_p	(s)	time from injection until breakthrough curve has reached peak concentration (peak time)
V	(m^3)	volume
v	(m/s)	flow velocity
$\bar{v}$	(m/s)	average velocity

x	(m)	distance in flow direction
θ_d		diffusion porosity
θ_e		effective porosity
θ_k		kinematic porosity
θ_r		residual porosity
θ_T		total porosity
ν	(m^2/s)	kinematic viscosity
δ	(kg/m^3)	bulk density

9. BIBLIOGRAPHY

Almén, K-E., Ekman, L., Olkiewicz, A. 1978: Försöksområdet vid Finnsjön. Beskrivning till berggrunds- och jordartskartorna. SKBF-KBS Teknisk rapport 79-02.

Bear, J. 1979: Hydraulics of Groundwater, Mc GRAW-HILL, Israel.

Carlsson, L., Gidlund, G., Hansson, K. och Klockars, C-E. 1979: Estimation of hydraulic conductivity in Swedish Precambrian crystalline bedrock. OECD-NEA, Workshop Mars 1979, Paris.

Danielsson, A. and Lindblom, P. 1976: The IDES system- An Image Dissector Echelle Spectrometer system for spectrochemical analysis. In Applied Spectroscopy, Vol. 30. No 2. 1976.

Darcy, H. 1856: Les Fontaines publiques de la ville de Dijon. Paris.

Davis, S. N., Thompson, G. M., Bentley, H. W., Stiles, G. 1980: Ground-water tracers- a short review. Ground Water, Volume 18, Number 1.

Duran, O., Magnusson, K-Å. 1980: Borrhålsmätningar av temperatur, SP, pH, Eh och borrhålsvätskans resistivitet. Delrapport, Prav 4.15.

Fried, J. J. 1975: Groundwater pollution. Elsevier, Amsterdam - Oxford - New York.

Gidlund, G., Hansson, K. och Thoregren, U. 1979: Kompletterande permeabilitetsmätningar i Karlshamnsområdet. KBS, Teknisk rapport, Nr 79-06, Stockholm.

Goblet, P., Ledoux, G., de Marsily, G., Peaudecerf, P., Calmels, P., Guizerix, R. 1980: Processes of solute transfer in fissured aquifers.

Klockars, C-E., Persson, O. 1978: Berggrundvattenförhållanden i Finnsjöområdets nordöstra del. KBS Teknisk rapport 60.

Klotz, D., Moser, H. 1974: "Hydrodynamic dispersion as aquifer characteristic: model experiments with radioactive tracers", Isotope Techniques in Groundwater Hydrology 1974 (Proc. Symp. Vienna, 1974), IAEA, Vienna.

Landström, O., Klockars, C-E., Holmberg, K-E och Westerberg, S. 1978: In situ experiments on nuclide migration in fractured crystalline rocks. KBS Teknisk rapport 110, Stockholm.

Lenda, A. och Zuber, A. 1970: Tracer dispersion in groundwater experiments. Proceedings of a symposium arranged by IAEA, Vienna.

Moye, D. G. 1967: Diamond drilling for foundation exploration. Civ. Eng. Trans., Vol. CE 9, No 1, Sydney.

Neretnieks, I. 1977: Retardation of espacing nuclides from a final depository. KBS Teknisk rapport 30, Stockholm.

Neretnieks, I. 1978: Transport of oxidants and radionuclides through a clay barrier. KBS Teknisk rapport 79, Stockholm.

Neretnieks, I. 1980: A note on dispersion mechanisms in the ground.

Norton, D. och Knapp, R. 1977: Transport phenomena in hydrothermal systems: The nature of porosity. Emer. Journal of Science, Vol. 277, sid 913 - 936.

Ogata, A., Banks, R. 1961: A Solution of the Differential Equation of Longitudinal Dispersion in Porous Media, US Geol. Surv. Prof. Paper 411-A, Washington.

Olkiewicz, A., Scherman, S., Kornfält, K-A. 1979: Kompletterande berggrundsundersökningar inom Finnsjö- och Karlshamnsområdena. SKBF-KBS Teknisk rapport 79-05.

Scherman, S. 1978: Förarbeten för platsval, berggrundsundersökningar. KBS Teknisk rapport 60.

SGU, 1979: Hydrauliska barriäregenskaper hos marknära bergmassor. Rapport utarbetad på uppdrag av PRAV. (Rapport Prav 1.24).

SGU, 1979: Beräkning av föroreningsspridning - processer - kvantifiering - modellanalys. Rapport utarbetad på uppdrag av Statens Naturvårdsverk, Uppsala.

Snow, D. T. 1968: Rock fracture spacings, openings and porosities. J. Soil Mech. Found. Div. Proc. ASCE, Vol. 94, No SM 1.

Zuber, A. 1974: "Theoretical possibilities of the two-well pulse method", Isotope Techniques in Groundwater Hydrology 1974 (Proc. Symp. Vienna, 1974), IAEA, Vienna.

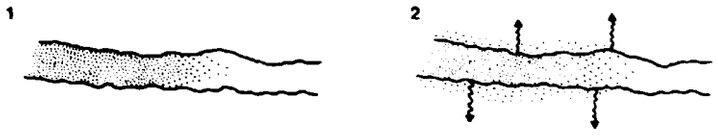

Fig. 3.3.2a

1) Diffusion in the groundwater of water-soluble substance in a water-bearing fracture.

2) Diffusion in the groundwater within the water-bearing fracture and into micro-fissures in the groundwater-bearing medium's matrix.

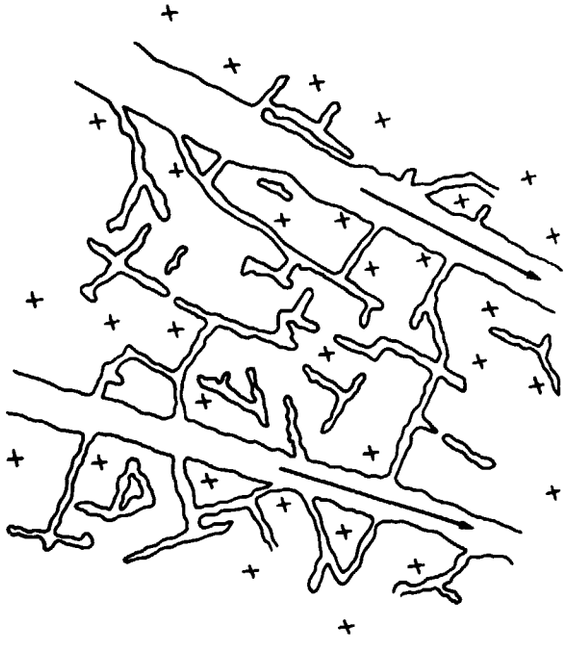

Fig. 3.3.2b

Schematic diagram of different fractures and their geometric relationships. The fractures that constitute the kinematic porosity and through which water flow takes place are marked with arrows. The interconnected small fractures constitute the diffusion porosity, while other fractures constitute the residual porosity (after Norton and Knapp, 1977).

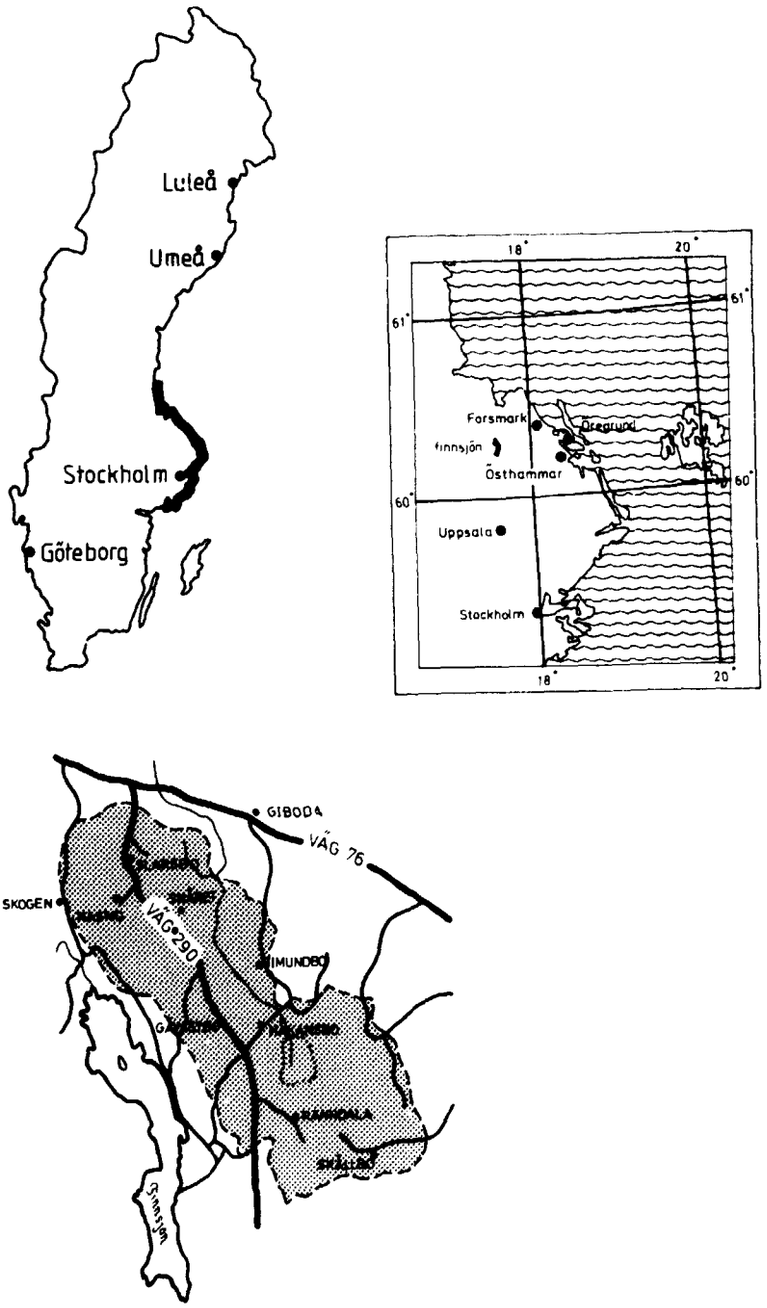

Fig. 4.1a Map showing location of Finnsjö field research area.

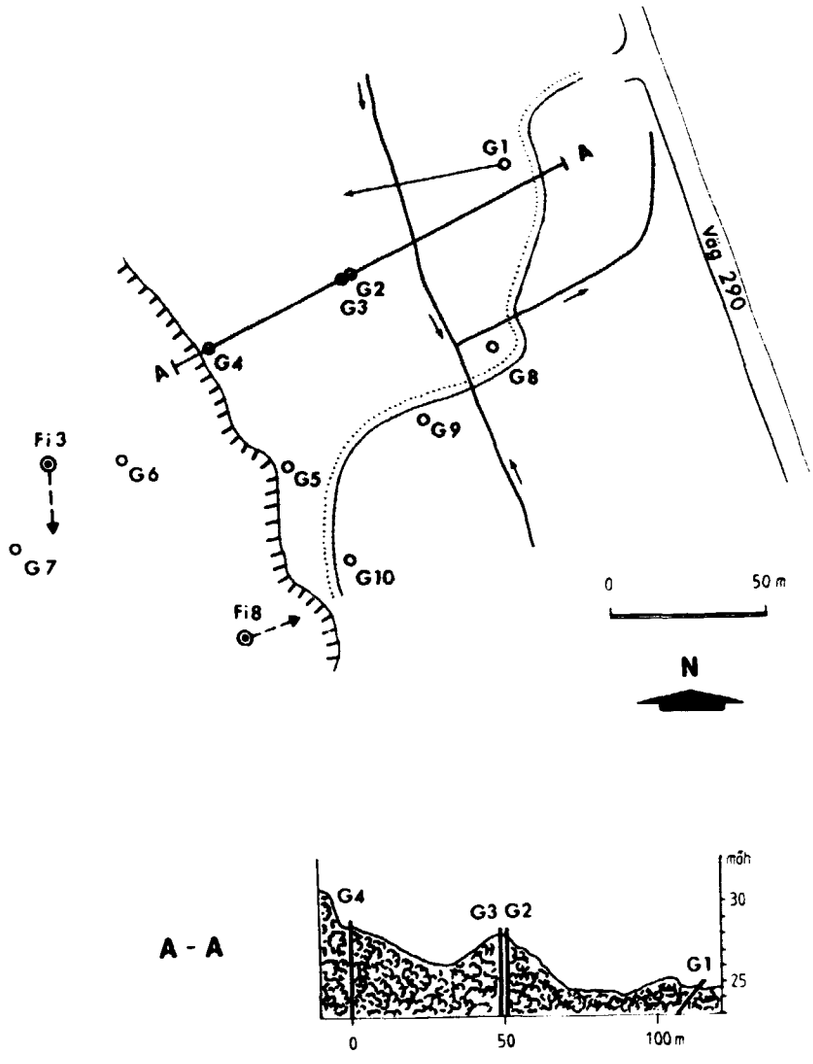

Fig. 4.2.1a Schematic map of test site showing location of boreholes.

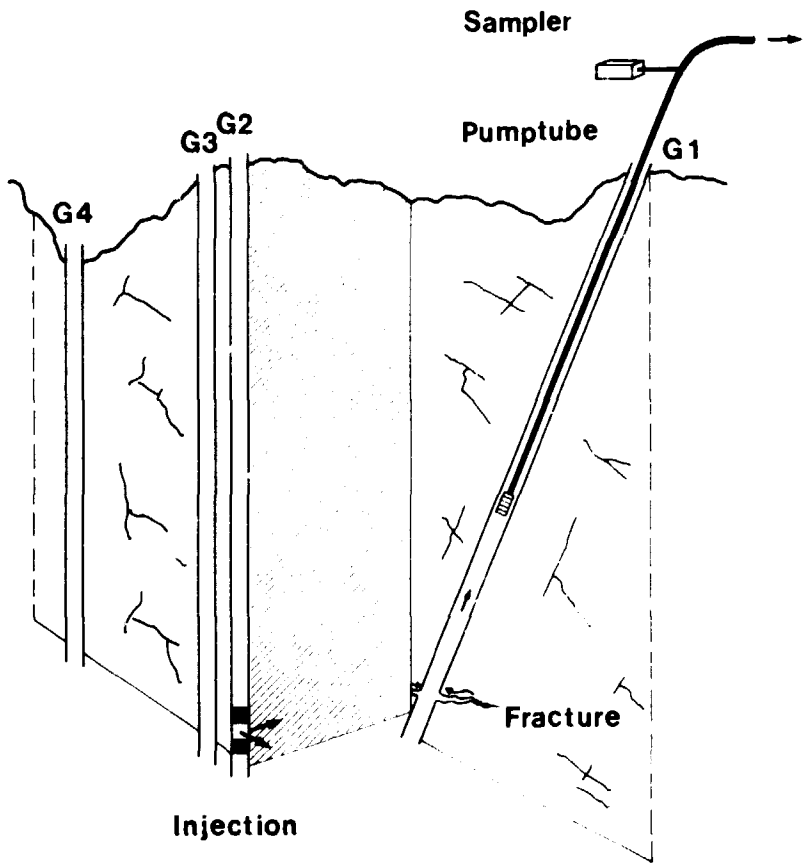

Fig. 5.3.1a Cutaway view of test site and instrument set-up.

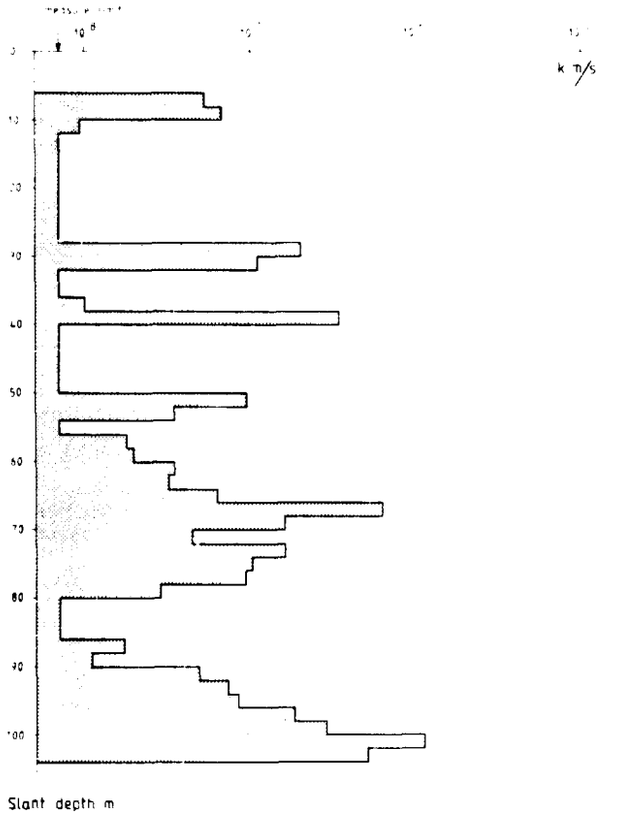

Fig. 6.1a Hydraulic conductivity as a function of borehole length for borehole G1.

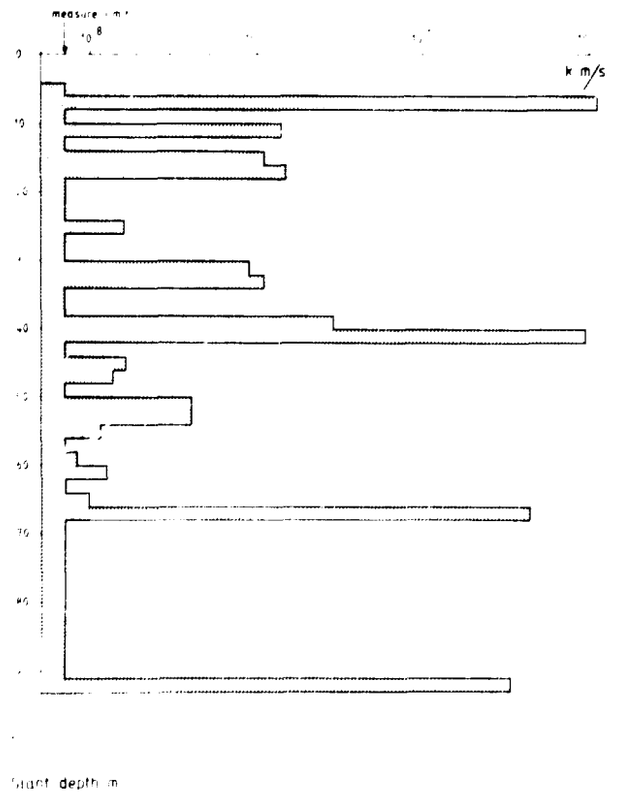

Fig. 6.1b Hydraulic conductivity as a function of borehole length for borehole G2.

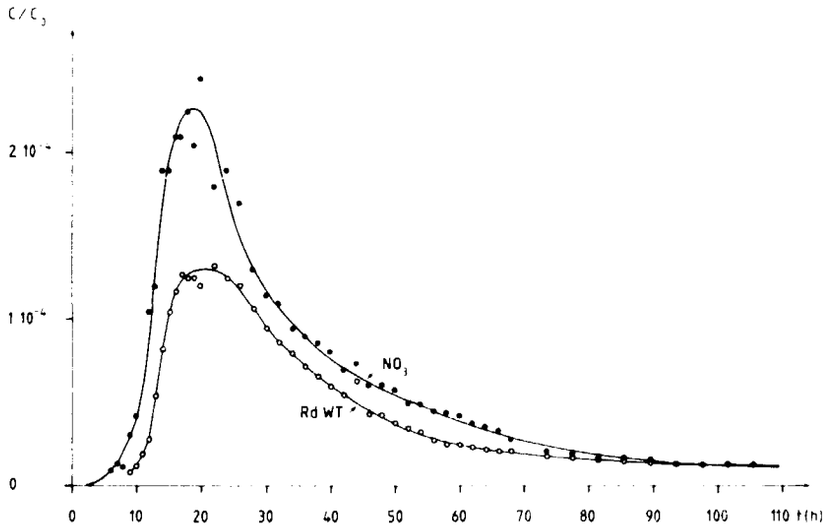

Fig. 6.2.1a Breakthrough curves for NO_3^- and RdWT in test 1.

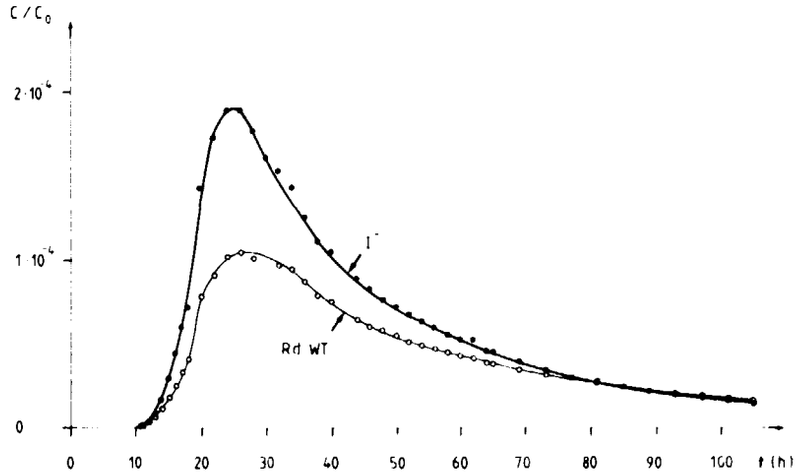

Fig. 6.2.1b Breakthrough curves for I^- and RdWT in test 2.

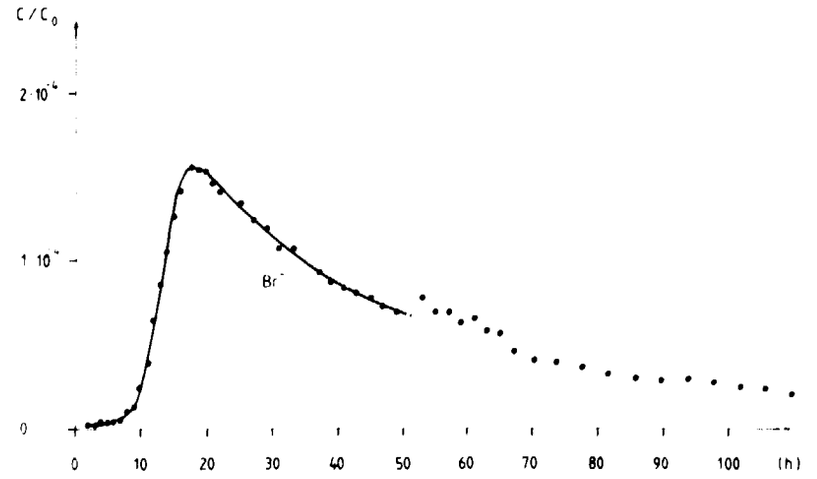

Fig. 6.2.1c Breakthrough curve for Br^- in test 3.

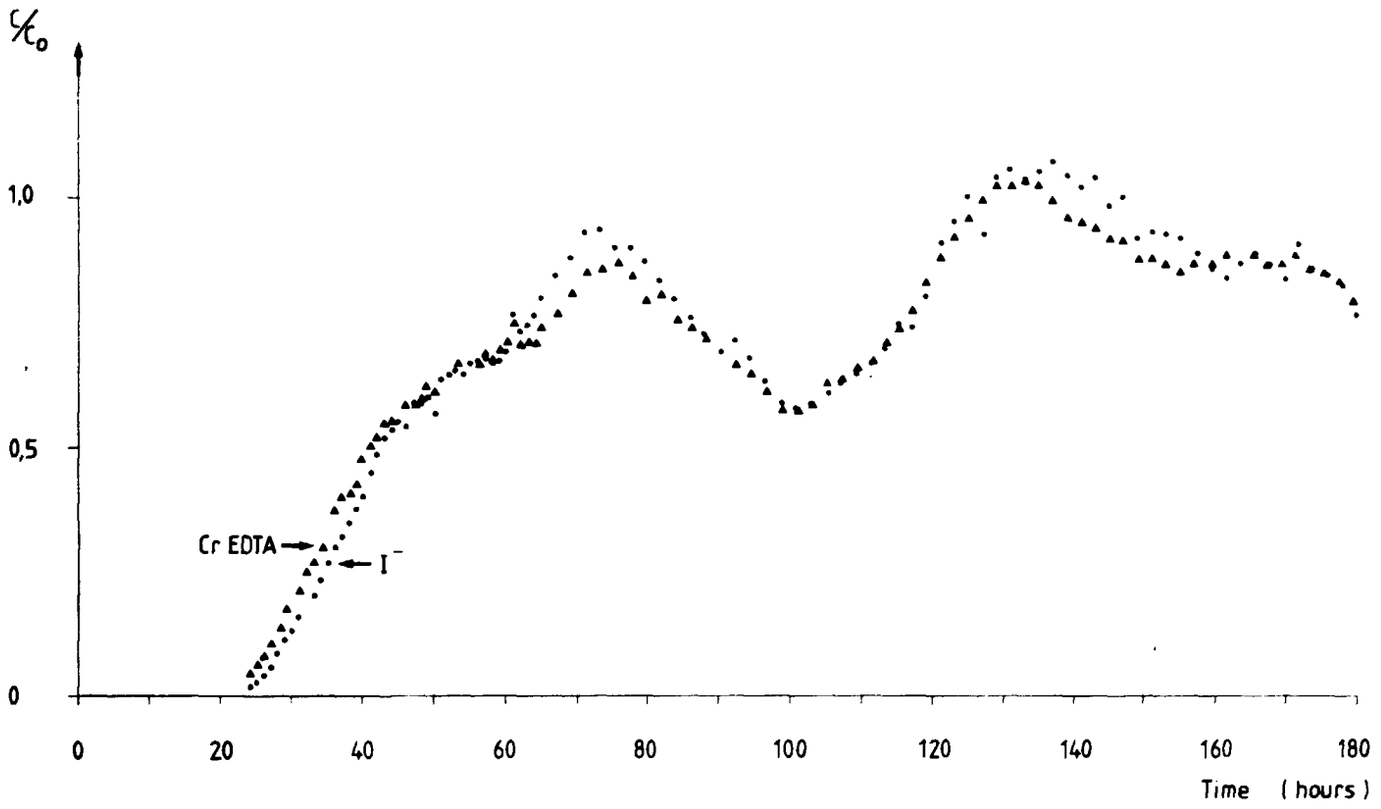

Fig. 6.2.1d Breakthrough curves for Cr-EDTA and I^- in test 4.

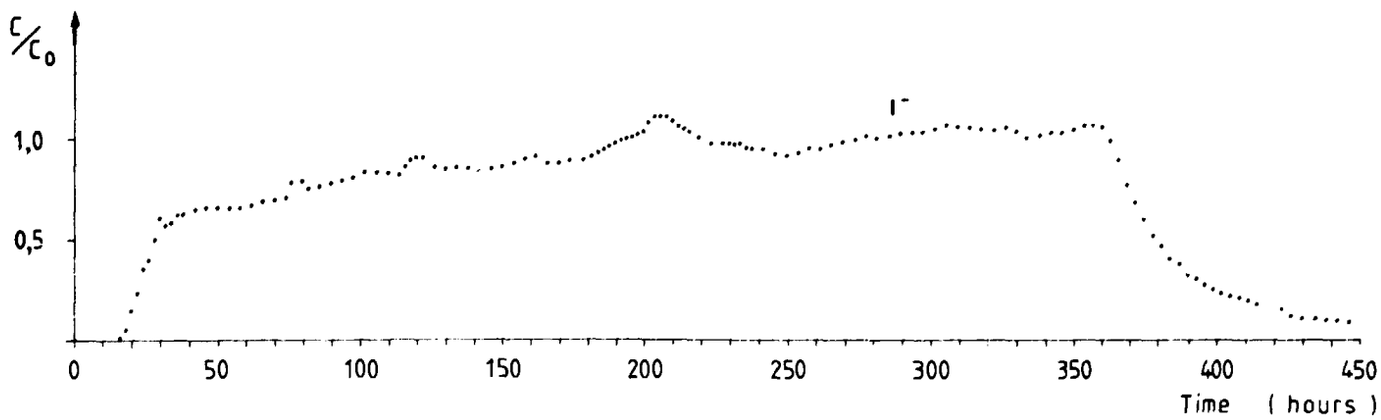

Fig. 6.2.1e Breakthrough curve for I^- in test 5.

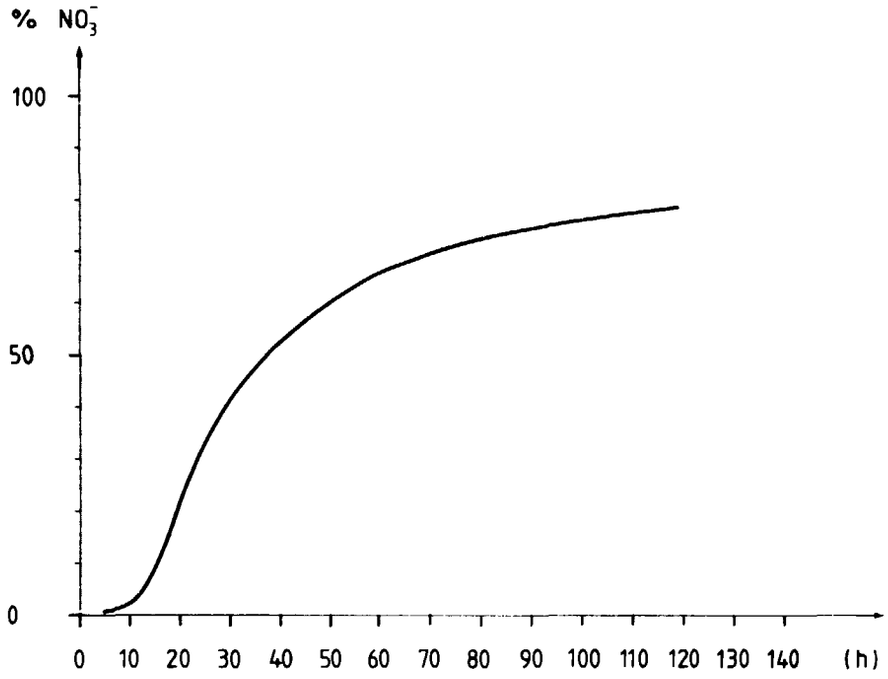

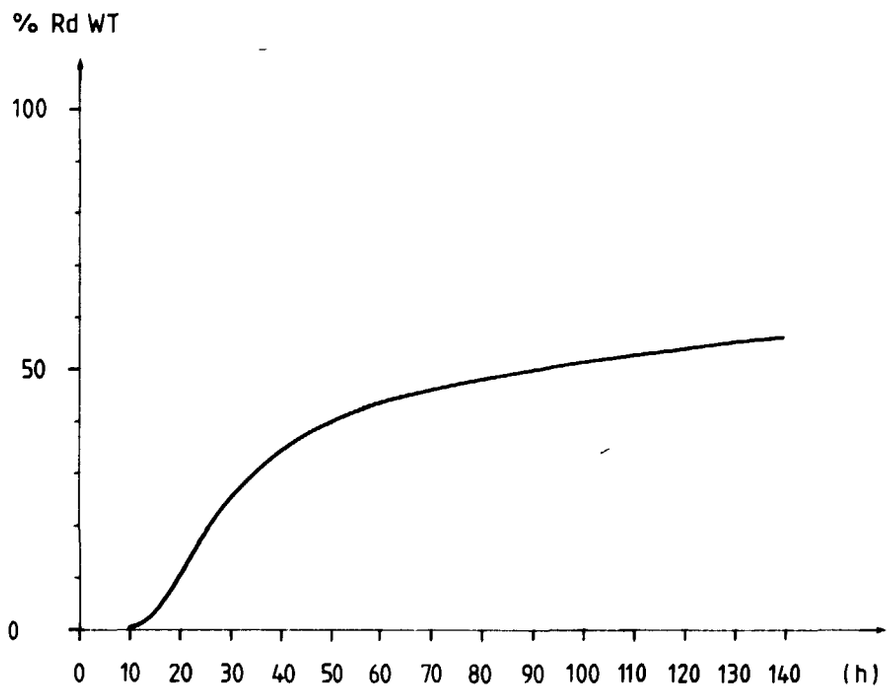

Fig. 6.2.1f *Recovery curves for NO_3^- and RdWT in test 1.*

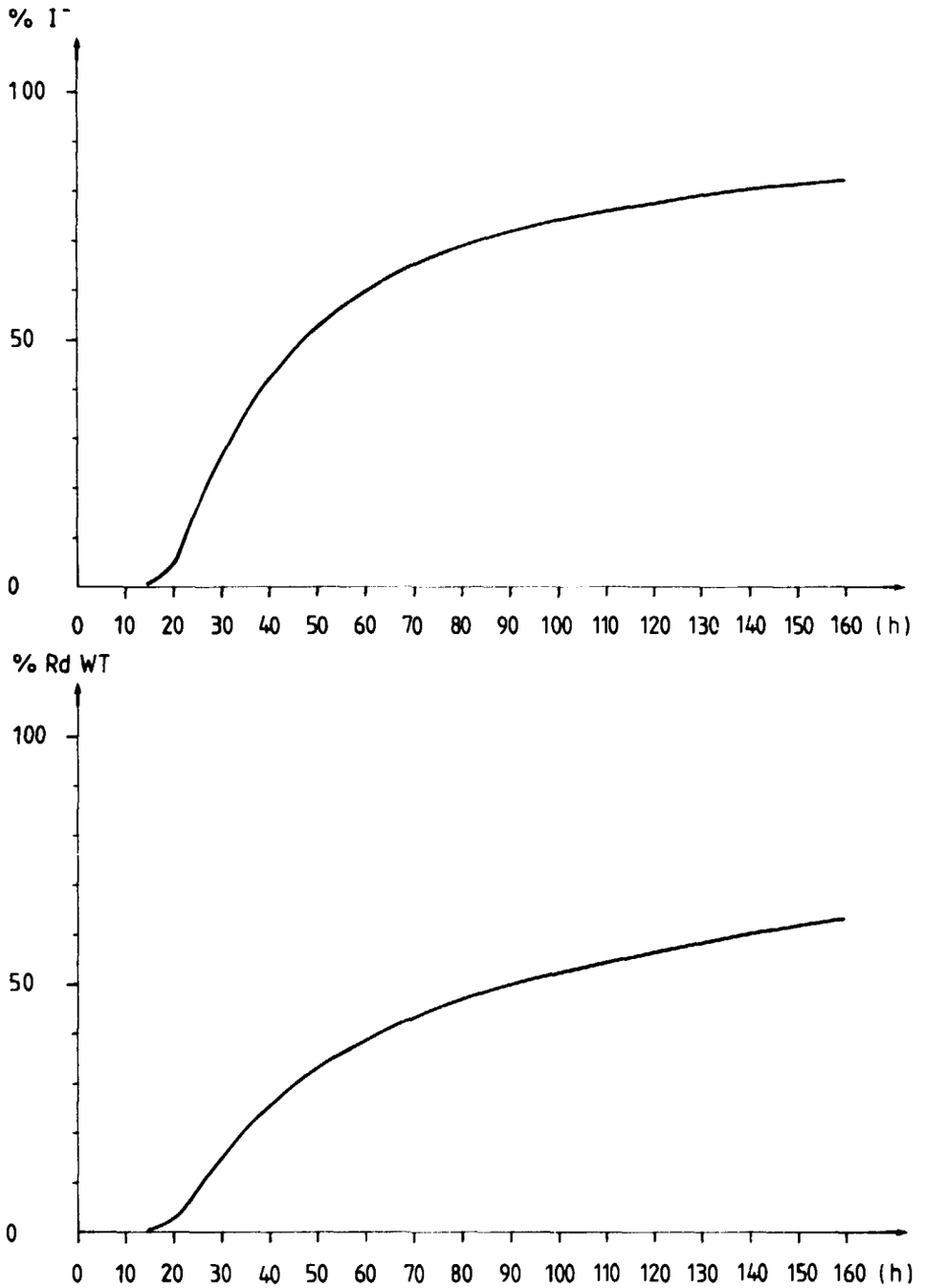

Fig. 6.2.1g Recovery curves for I^- and RdWT in test 2.

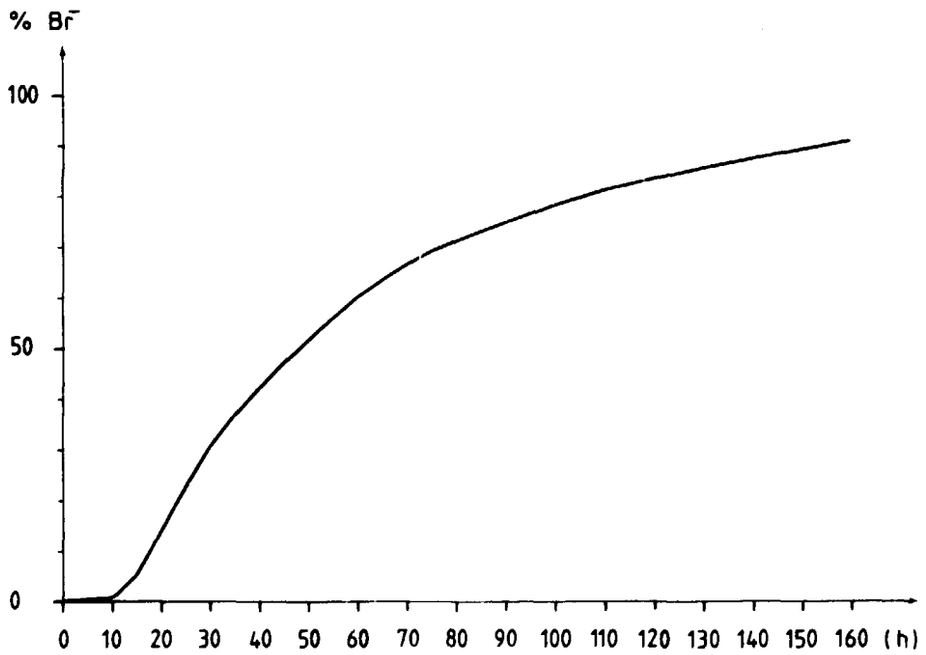

Fig. 6.2.1h Recovery curve for Br^- in test 4.

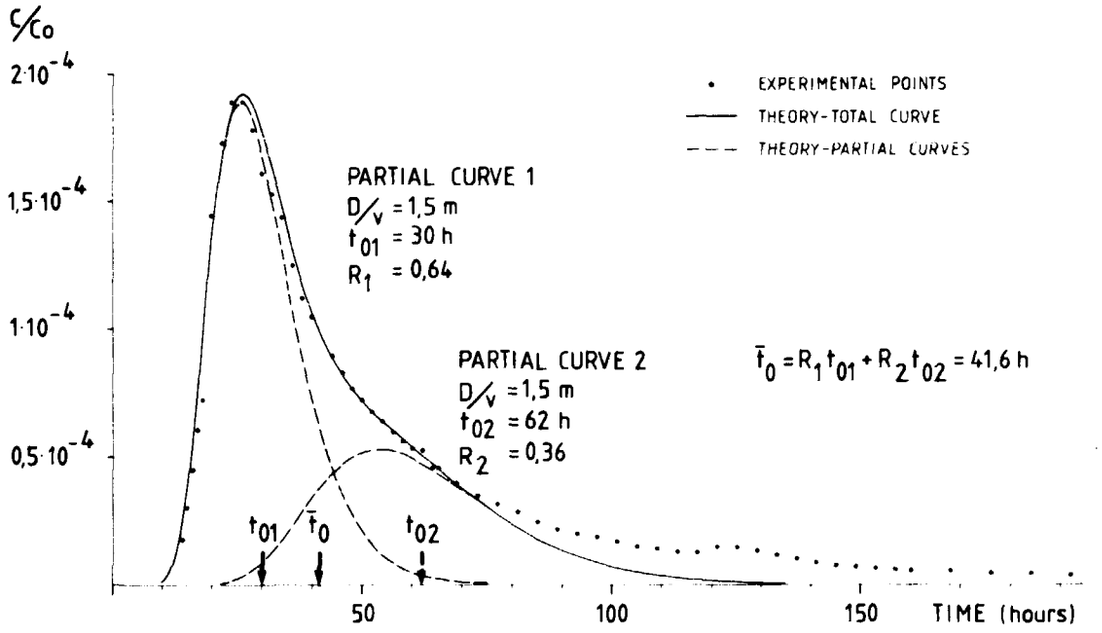

Fig. 6.2.3a *Experimental breakthrough curve for I^- in test 2 and fit with two theoretical curves.*

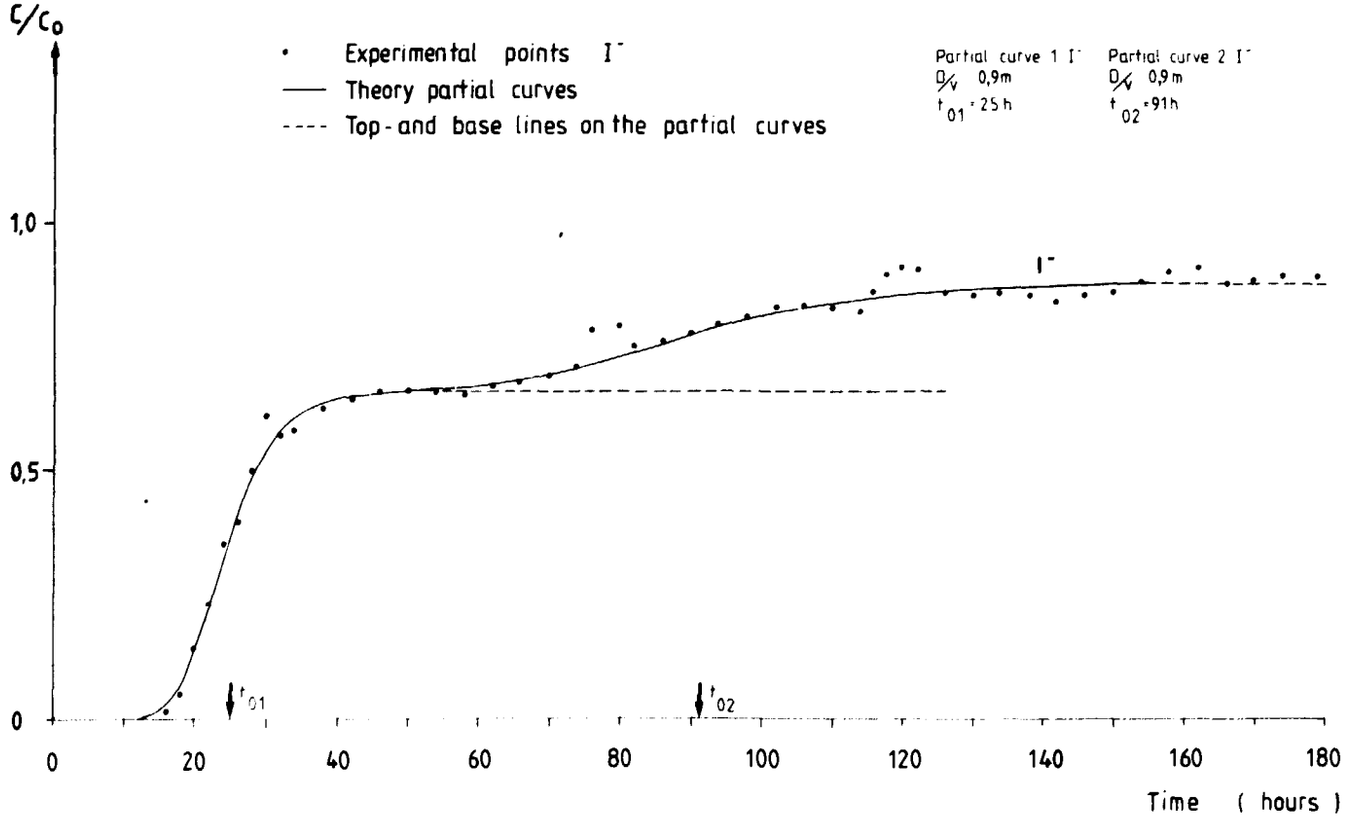

Fig. 6.2.3b *Experimental breakthrough curve for I^- in test 5 and fit with two theoretical curves.*

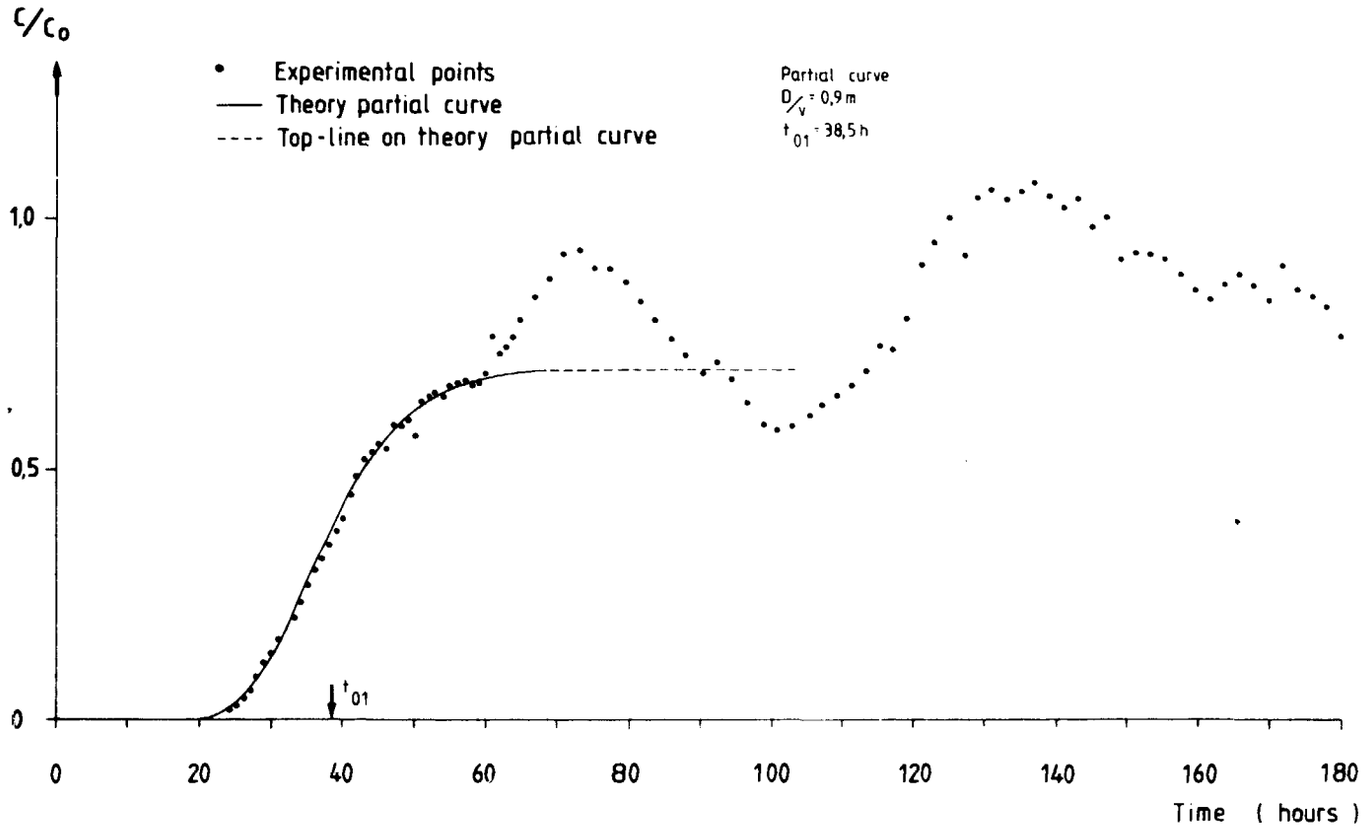

Fig. 6.2.3c *Experimental breakthrough curve for I^- in test 4 and fit with a theoretical curve.*

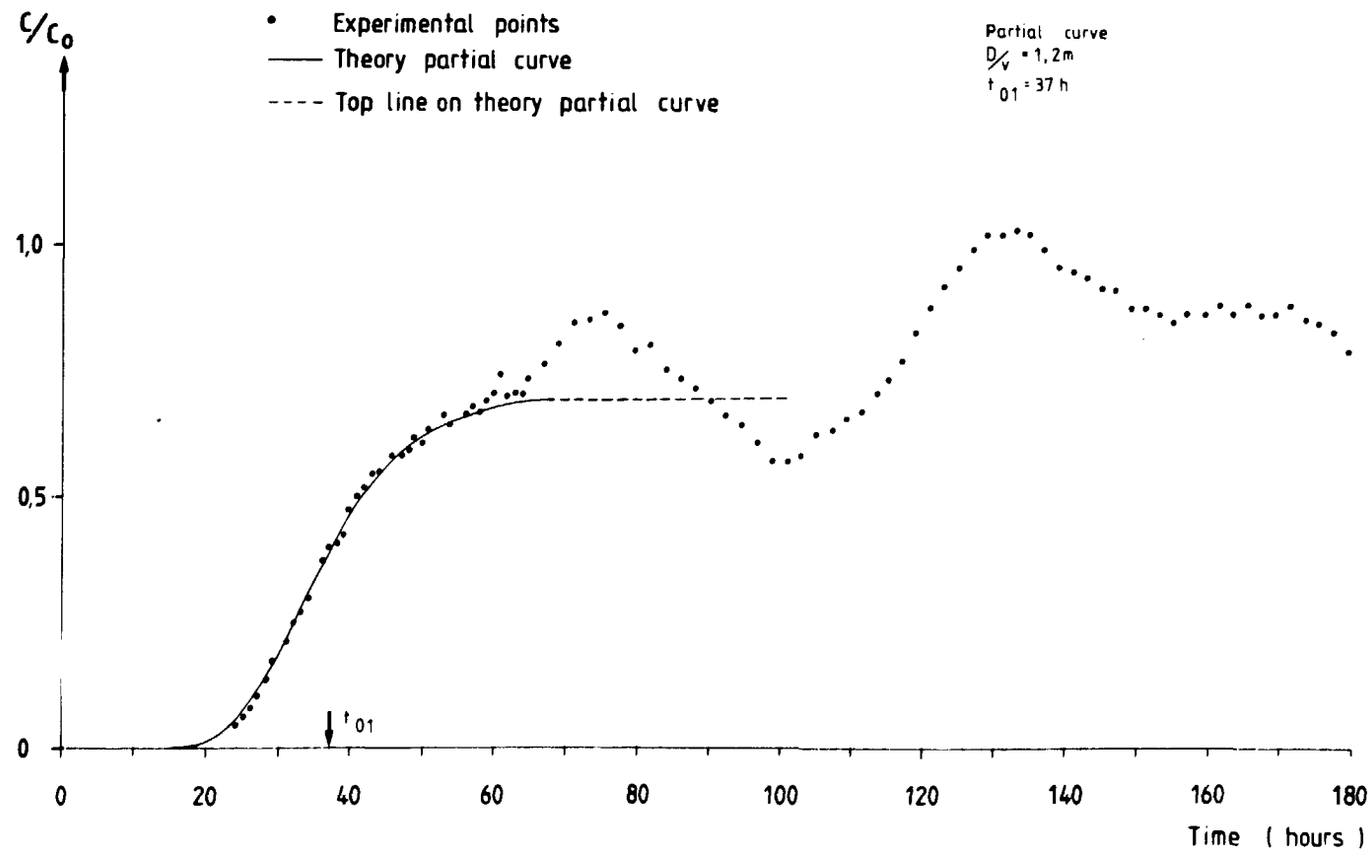

Fig. 6.2.3d *Experimental breakthrough curve for Cr-EDTA in test 4 and fit with a theoretical curve.*

FÖRTECKNING ÖVER KBS TEKNISKA RAPPORTER

1977-78

TR 121 KBS Technical Reports 1 - 120.
Summaries. Stockholm, May 1979.

1979

TR 79-28 The KBS Annual Report 1979.
KBS Technical Reports 79-01--79-27.
Summaries. Stockholm, March 1980.

1980

TR 80-26 The KBS Annual Report 1980.
KBS Technical Reports 80-01--80-25.
Summaries. Stockholm, March 1981.

1981

TR 81-01 A note on dispersion mechanisms in the ground
Ivars Neretnieks
Royal Institute of Technology, March 1981

TR 81-02 Radiologisk exponering från strandsediment innehållande torium-229
Karl Anders Edvardsson
Sverker Evans
Studsvik Energiteknik AB, 1981-01-27

TR 81-03 Analysis of the importance for the doses of varying parameters in the biopath-program
Ulla Bergström
Studsvik Energiteknik AB, 1981-03-06

TR 81-04 Uranium and radium in Finnsjön - an experimental approach for calculation of transfer factors
Sverker Evans
Ronny Bergman
Studsvik Energiteknik AB, 1981-05-07

TR 81-05 Canister materials proposed for final disposal of high level nuclear waste - a review with respect to corrosion resistance
Einar Mattsson
Swedish Corrosion Institute, Stockholm, June 1981

TR 81-06 Ion diffusion through highly compacted bentonite
Trygve Eriksen
Department of Nuclear Chemistry
Royal Institute of Technology, Stockholm
Arvid Jacobsson
Roland Pusch
Division Soil Mechanics, University of Luleå
1981-04-29

TR 81-07 Studies on groundwater transport in fractured crystalline rock under controlled conditions using nonradioactive tracers
Erik Gustafsson
Carl-Erik Klockars
Geological Survey of Sweden, Uppsala, April 1981

TR 81-08 Naturligt förekommande uran-, radium- och radonaktiviteter i grundvatten
Mats Aastrup
Sveriges Geologiska Undersökning oktober 1981

ISSN 0348-7504